AVERAGE CURRENT-MODE CONTROL

A thesis submitted in partial fulfillment

of the requirements for the degree of

Master of Science in Electrical Engineering

By

Ankit Chadha

B. S., Koneru Lakshmaiah University, Guntur, Andhra Pradesh, India, 2013

2015

Wright State University

WRIGHT STATE UNIVERSITY
GRADUATE SCHOOL

January 5, 2016

I HEREBY RECOMMEND THAT THE THESIS PREPARED UNDER MY SUPERVISION BY Ankit Chadha ENTITLED Average Current-Mode Control BE ACCEPTED IN PARTIAL FULFILLMENT OF THE REQUIREMENTS FOR THE DEGREE OF Master of Science in Electrical Engineering.

Marian K. Kazimierczuk, Ph.D.
Thesis Director

Brian Rigling, Ph.D.

Chair
Department of Electrical Engineering
College of Engineering and
Computer Science

Committee on
Final Examination

Marian K. Kazimierczuk, Ph.D.

Yan Zhuang, Ph.D.

Lavern Alan Starman, Ph.D.

Robert E. W. Fyffe, Ph.D.
Vice President for Research and
Dean of the Graduate School

ABSTRACT

Chadha, Ankit. M.S.E.E, Department of Electrical Engineering, Wright State University, 2016. *Average current-mode controller.*

In this thesis, an average current-mode controller is analyzed for controlling power electronic converters. This controller consists of two loops. An inner loop, which senses and controls the inductor current and an outer loop, which is used to control the output voltage and provide reference voltage for the inner current loop. An average current-mode controller averages out high frequency harmonics it senses from the inductor current to provide a smooth DC component. This can be used as a control voltage for a pulse width modulator and produce switching pulses for the power electronic converters. An average current-mode controller can also be designed for a good bandwidth, which helps in accurate tracking of the sensed inductor current.

For a better understanding of the operation of an average current-mode controller analytical equations are derived. Many transfer functions, which help analyze the properties of an open loop system, the controller transfer functions and a block diagram representing the converter along with current and voltage-control loops are presented. The block diagram and the transfer functions were used to derive the required controller parameters on MATLAB. The designed converter along with the controller is implemented on SABER circuit simulator. Waveforms representing the analytical equations along with the dynamic properties of the converter with the controller were plotted.

The plotted SABER simulations were in agreement with the analytical equations. The designed controller was able to produce a controlled output voltage for step change in input voltage and load resistance, when simulated on SABER. Ripples could be observed in the control voltage of the controller, when designed for a good bandwidth. This was also represented by the derived analytical equations.

Contents

1 Introduction **1**

1.1 Thesis Objectives 3

1.2 Thesis Outline 4

2 Overview of Buck DC-DC converter **5**

2.1 Circuit operation of Buck DC-DC converter 5

2.2 Small-Signal Model of a Buck DC-DC Converter 6

2.3 Open-Loop Control-to-Output Voltage Transfer Function 7

2.4 Open-Loop Control-to-Inductor Current Transfer Function 10

2.5 Open-Loop Input-to-Output Voltage Transfer Function 15

2.6 Open-Loop Input Impedance Transfer Function 17

2.7 Open-Loop Output Impedance Transfer Function 19

3 Controllers **22**

3.1 Introduction 22

3.2 Voltage-Mode Control 22

3.2.1 Proportional Controller 23

3.2.2 Differentiator 24

3.2.3 Integrator 25

3.3 Current-Mode Control 26

3.3.1 Peak Current-Mode Control 27

3.3.2 Average Current-Mode Control 28

4 Design **36**

4.1 Introduction 36

4.2 Design of an Open-Loop Buck DC-DC Converter in Continuous Conduction Mode 36
4.3 Closed-Loop Buck DC-DC Converter 41
4.3.1 Design of Inner Current Control-Mode-Controller 44
4.3.2 Design of Outer Voltage-Mode-Controller 54

5 Saber Simulations and Results **62**
5.1 Introduction 62
5.2 Dynamic Response of Inner Current Control Loop 62
5.2.1 Controller Response 64
5.2.2 Dynamic Response of the Buck DC-DC Converter with Inner Current Control Loop for the Step Change in Load Resistance . . 67
5.2.3 Dynamic Response of the Buck DC-DC Converter with Inner Current Control for the Step Change in Input Voltage 67
5.3 Dynamic Response of Outer Voltage Control Loop 68
5.3.1 Dynamic Response of the Buck DC-DC Converter with Inner Current and Outer Voltage Control Loop for the Step Change in Load Resistance 70
5.3.2 Dynamic Response of the Buck DC-DC Converter with Inner Current and Outer Voltage Control Loop for the Step Change in Input Voltage 70

6 Conclusion **72**
6.1 Summary 72
6.2 Future Work 72

7 Bibliography **73**

List of Figures

2.1 Circuit diagram of a buck DC-DC converter[5] 5

2.2 Small-signal model of a buck DC-DC converter. 6

2.3 Small-signal model of a buck DC-DC converter to derive control-to-output voltage transfer function 7

2.4 Corner frequency as a function of load resistance 12

2.5 Damping factor as a function of load resistance 13

2.6 Idealized Bode plots of the open-loop control-to-inductor current transfer function T_i for the buck converter 14

2.7 Small-signal model of a buck DC-DC converter to derive input-to-output voltage transfer function 15

2.8 Small-signal model of a buck DC-DC converter to derive output impedance 19

3.1 Block diagram of an op-amp as a controller 23

3.2 Circuit diagram of a proportional controller 24

3.3 Circuit diagram of a differentiator 24

3.4 Circuit diagram of an integrator 25

3.5 Block Diagram representing a general current control scheme 26

3.6 Circuit diagram of a peak current-mode controller[5] 27

3.7 Circuit diagram of an average current-mode control 28

3.8 (a) Waveform of inductor current of a buck DC-DC converter. (b) Waveform of control voltage of a pulse-width modulator which is an amplified version of the sensed inductor current. 31

3.9 (a) Waveform of inductor current of a buck DC-DC converter. (b) Waveform of control voltage of a pulse-width modulator when cross over frequency of the controller is less than the switching frequency of the buck DC-DC converter. 31

3.10 (a) Waveform of inductor current of a buck DC-DC converter. (b) Waveform of control voltage of a pulse-width modulator when cross over frequency of the controller is higher than the switching frequency of the buck DC-DC converter. 32

3.11 Magnitude and phase plot of a first order type one average current-mode controller 33

3.12 Waveforms in the pulse-width modulator representing the sawtooth voltage v_t, the control voltage v_{C1} and gate-to-source voltage v_{GS} for controller crossover frequency less than the switching frequency.[5] 34

3.13 Waveforms in the pulse-width modulator representing the sawtooth voltage v_t, the control voltage v_{C1} and gate-to-source voltage v_{GS} for controller crossover frequency more than the switching frequency. 35

4.1 Circuit diagram of the buck DC-DC converter after implementing the design specification. 38

4.2 Magnitude and phase plots of control-to-inductor current transfer function of buck DC-DC converter. 40

4.3 Step response of inductor current of buck DC-DC converter for a step change in duty cycle. 41

4.4 Block diagram of the DC-DC buck converter with inner current control loop and output voltage control loop. 42

4.5 Circuit diagram of DC-DC buck converter with inner current control loop and output voltage control loop 43

4.6 Block diagram of inner loop representing closed loop inductor current to control relationship 44

4.7 Magnitude and phase plots of internal loop gain without controller compensation. 45

4.8 Circuit diagram of a first order type zero current mode controller 47

4.9 Magnitude and phase plots of average current mode controller 50

4.10 Magnitude and phase plots of inner loop gain with controller 51

4.11 Block diagram of inner closed loop buck DC-DC converter. 52

4.12 Magnitude and phase plots of closed loop control-to-inductor current transfer function of buck DC-DC converter. 53

4.13 Step response of inductor current of a closed-loop buck DC-DC converter for a step change in duty cycle 54

4.14 Circuit diagram representing PI controller for outer voltage loop control. 55

4.15 Block diagram representing outer loop gain 57

4.16 Magnitude and phase plots of outer loop gain with controller. 58

4.17 Block diagram for closed loop gain of outer voltage loop control. 59

4.18 Magnitude and phase plots of outer closed loop gain with controller. 60

4.19 Step response of outer closed loop with controller. 61

5.1 Saber circuit for average current mode control of inductor current. 63

5.2 Waveforms representing control and sawtooth reference voltages for a good phase margin. 65

5.3 Waveforms representing control and sawtooth reference voltage with high capacitance in the feedback of the controller. 66

5.4 Waveforms representing inductor current and output voltage of the buck DC-DC converter for a step change in load resistance. 67

5.5 Waveforms representing inductor current and output voltage of the buck DC-DC converter for a step change in input voltage. 68

5.6 Saber circuit of a buck DC-DC converter with both inner current control and outer voltage control. 69

5.7 Waveforms of inductor current and output voltage of the buck DC-DC converter for a step change in load resistance. 70

5.8 Waveforms of inductor current and output voltage of the buck DC-DC converter for a step change in input voltage. 71

Acknowledgement

To start of, I would like to express my immense gratitude to my advisor Dr. Marian K. Kazimierczuk, whose support, motivation and wisdom has helped me through out my research. I would also like to thank my thesis committee members Dr. Yan Zhuang and Lavern Alan Starman for their insightful comments and suggestions. I am grateful to the Department of Electrical Engineering and the Department Chair, for giving me this opportunity to obtain my MS degree at Wright State University. A sincere thanks also goes to my fellow colleague Agasthya Ayachit, whose support and experience built the confidence in me. Last but not the least I would like to thank my family, who stood by me on every decision I made and who have always showed me the right path.

1 Introduction

Obtaining a sustainable energy production at lowered costs has always been a global priority. This has lead to many improvements in technologies. Power electronic converters with their many available topologies, which help interface different energy sources is an example of one such technology. Power electronic converters use MOSFETs, driven by pulse width modulated (PWM) pulses, as switches to produce output voltage. Hence, they are named switch-mode DC-DC converters. The turn-on time and the turn-off time of these switches play an important role deciding the characteristics of the converter as they provide conversion ratio for these converters. A similar stepping up or stepping down of the output voltage can be obtained by using a transformer with proper turns ratio. But, a transformer is usually responsible for high switching surges, which can damage the switching components in the circuit. Due to these features a great number of uses for DC-DC converters like, an integrated circuit utilizing a switching converter for a 3.3 V or 1.5 V or a power supply for automobile industries for electronic load, have emerged [13].

Since power electronic converters provide good conversion ratio, a proper regulation of the duty cycle can help in controlling the output voltage. A controller can be employed for such application. The main task of a controller is to sense a change in a required quantity and provide proper compensation, when the situations asks for it. Power electronic converters like, a DC-DC buck or a DC-DC boost converter employ such controllers to keep the output voltage in desired range. Since a controller senses and controls a required parameter, multiple control circuits can be employed to satisfy the multiple application requirement. A current mode controller is an example of one such controller, where the controller senses the current instead of a voltage and provides the required compensation. Both, the current mode and the voltage mode controller can be applied to power electronic converters and if required multiple loops

containing both the types of control can also be integrated onto a circuit.

Adopting a current mode control usually has many advantages over voltage mode control. A current mode control has a faster transient response, provides over-current protection to a circuit and are also easier to design. Due to these advantages a current-mode control is a preferable option in power supply industries. There are many types of current-mode-control available like average, peak, valley current-mode control in which, the sensed current is converted into voltage to compare it to a reference voltage and let the controller decide the required compensation.

A peak current mode control is a simple yet robust way to control a DC-DC power electronic converter. This control scheme uses an op-amp and a latch to decide the duty cycle of a converter. This is done by using a threshold voltage given to the sensed inductor current. Whenever the sensed inductor current reaches the given threshold voltage MOSFET is made to turn off and later the time period of the converter is completed by switching back the MOSFET on by using clock and a latch. Problem with this type of a current control is that, since it uses the peak value of the inductor current any harmonics in the system can cause false triggering by the controller. This is usually the case in power factor correction circuits.

An average current mode controller senses and averages out any surge in the sensed current and making it a better option, when trying to control a circuit with power factor correction. Since current spikes are common for such circuits. In average current mode control the sensed signal is first averaged out. Therefore, filtering any harmonics that could have been present in the inductor current. Also, average current mode control offers a higher low frequency gain thus, helps in tracking the current profile with high accuracy. An average current mode controllers gain compensation can be decided and designed depending on the controller requirements. In [8] and [2] two different types of average current mode control circuits have been used.

In [8] a buck converter is analyzed with a type one average current mode controller to control the inductor current with the control signal, which in this case is duty cycle. Doing so causes DC phase of the system to be -90^o. In this study, a first order type zero average current control circuit is used to control a buck converter for which the transfer function for the control-to-inductor current is derived. Using this transfer function required magnitude and phase plots are plotted, which helps to decide the required controller compensation and the controller parameters. The obtained control scheme with the buck converter is analyzed using MATLAB and Saber to note the dynamic properties of this controller.

1.1 Thesis Objectives

- Understand the difference between peak current mode control and average current mode control as it helps in better understanding of a current mode controller and how each of these controllers are implemented

- Derive different transfer functions namely, input voltage-output voltage transfer function (M_v), control-to-output voltage transfer function (T_p), output impedance (Z_o), input impedance (Z_i) and control-to-inductor current transfer function (T_i). This helps one to understand the open loop characteristics of the buck converter.

- Knowing the open loop characteristics of a buck converter gives knowledge about the compensation requirement of the converter by plotting for its loop gain without any controller compensation

- After obtaining the required controller design, buck along with the controller is connected and simulated on saber to observe the dynamic property of the converter and the control circuit.

1.2 Thesis Outline

This thesis is written in following order:

- Chapter 2: Working of a buck DC-DC converter is discussed. Followed by derivation of different transfer functions using it small-signal model obtained from circuit averaging method.

- Chapter 3: To be able to control the discussed converter in chapter 2 different types of controllers are summarized in here. This chapter mainly shed light on the working of the first order average current mode controller, which is the concentration of this thesis.

- Chapter 4: This chapter helps in obtaining all the required parameters for the converter to run and later control it. For this, the considered buck DC-DC converter is designed for the required specifications. Since, this control scheme has two controllers, a design procedure for our first order average current mode controller and finally, a design procedure for a voltage mode controller is mentioned.

- Chapter 5: In this chapter a powerful simulation tool namely, Saber is used to simulate the buck DC-DC converter with average current mode controller to observe its dynamic properties

2 Overview of Buck DC-DC converter

2.1 Circuit operation of Buck DC-DC converter

A buck converter as the name suggests helps in chopping or in other words steps down the applied input voltage. It uses the switching property of a MOSFET, diode and power storing property of an inductor in the form of current, to obtain such a drop in voltage. The circuit diagram representing a buck converter can be seen in Figure 2.1.

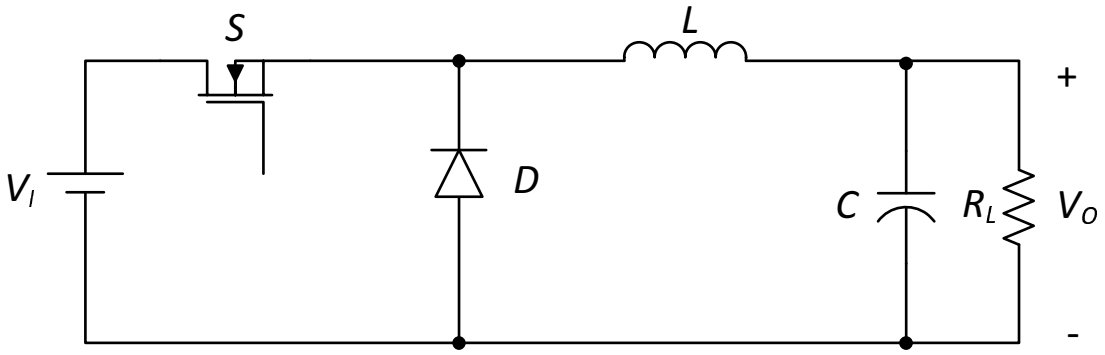

Figure 2.1: Circuit diagram of a buck DC-DC converter[5]

The converter starts working, when high gate-to-source voltage (V_{GS}) is applied to the MOSFET, which causes the MOSFET to switch on. At this point the MOSFET is short circuited. This builds up a reverse bias voltage across the diode forming an open circuit across the diode and the input voltage is being supplied to the load through the inductor. The capacitor connected as shown in Figure 2.1 filters out any AC component from the output voltage. This continues from time $t = 0$ till $t = DT$, where T is the total time period and D is the Duty cycle of the applied pulse to the MOSFET. After time $t = DT$, the V_{GS} applied to the MOSFET drops and is not enough to drive the MOSFET causing the MOSFET to switch off. This creates an open circuit by the MOSFET. At this point, the diode is forward biased by the output voltage. Now, the load is no longer supported by the input supply and the

energy stored in inductor in the form of current circulates within the system through the diode. Here the diode acts like a free wheeling diode. The point to be noted is that power falls due to this action and the output voltage is lower than the input. Thus, providing us with a lowered output voltage.

2.2 Small-Signal Model of a Buck DC-DC Converter

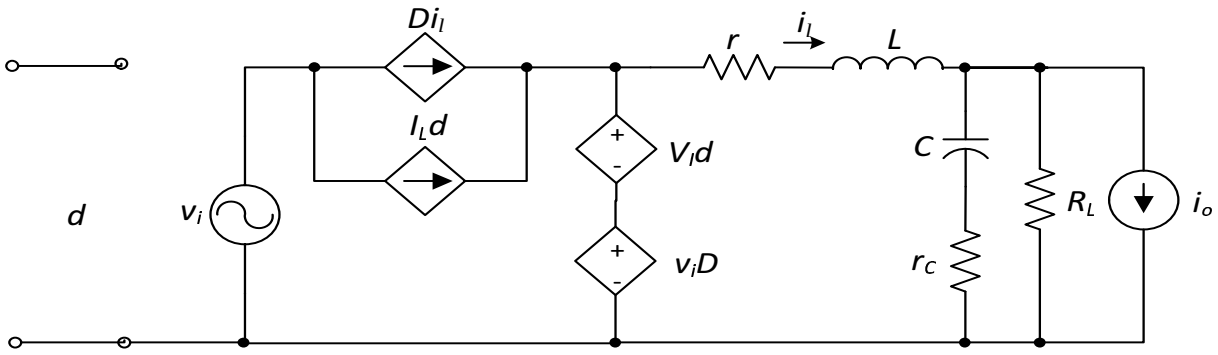

Figure 2.2: Small-signal model of a buck DC-DC converter.

The main interest for the design of a controller for a power electronic converters are its frequency response, transient response and stability for which one needs linear circuit theory. But, power converters are highly non-linear circuit. Therefore, such an analysis is not possible. For this, the circuit can be linearized by using circuit averaging method. In these circuits the switches used in the system can be replaced for a voltage or a current dependent sources. Also the DC voltage and current sources can be replaced by time varying AC components so that perturbations in the system can be represented. The on-state resistances are also taken into consideration. The circuit hence is called a large signal model. Since, the magnitude of small-signal model is low enough, the large signal model can be further simplified by neglecting the products of AC components to form a low frequency small-signal model. A small-signal model of a buck converter can be seen in Figure 2.2. The following assumptions are to be made to obtain such a circuit:

- Neglect switching losses, that is neglect the output capacitance of a transistor and diode capacitance.
- Transistor and diode in off-state does not allow any current to flow, that is the off-state resistance is infinite.
- Transistor in its on-state acts as a linear time invariant resistor, while the diode in its on-state can be represented as a voltage source V_F in series with a linear time invariant resistor.

2.3 Open-Loop Control-to-Output Voltage Transfer Function

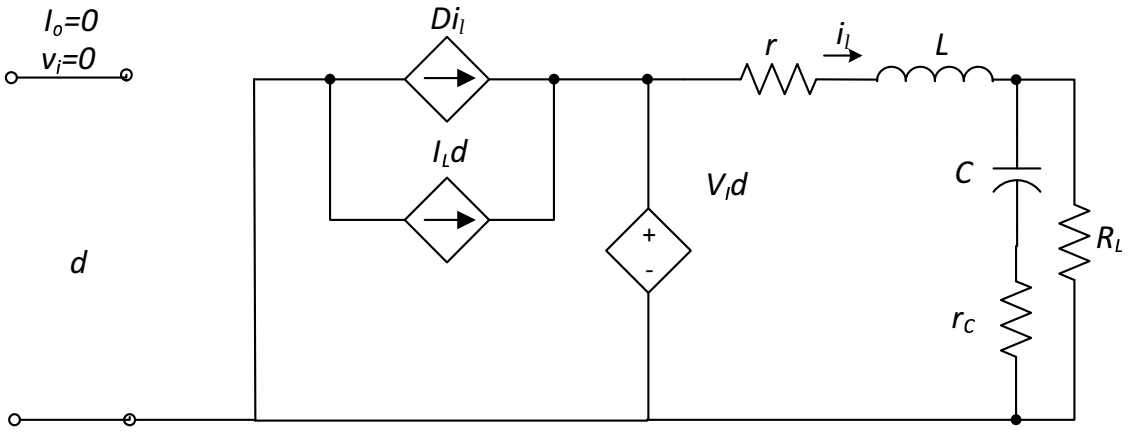

Figure 2.3: Small-signal model of a buck DC-DC converter to derive control-to-output voltage transfer function

A buck converter is designed for a constant output voltage but due to uncertain disturbances in the system like change in load or a surge in supply, the output voltage of the system might rise or fall, which needs to be checked by using a controller. A transfer function helps in relating a signal which is to be controlled and a control signal. Doing so aids in understanding how the system behaves in certain conditions. A control-to-output voltage transfer function is an example of one such transfer function. A control-to-output voltage transfer function as the name suggests provides a

transfer function or in layman's term provides a relation between control and output voltage, where the control signal is the duty cycle. Now, knowing such a relation will help us describe characteristics for the required controller and hence, design one. From Figure 2.2, let us assume that the perturbations in the system due to input voltage v_i and output current i_o are zero which is depicted in Figure 2.3.

From Figure 2.3, Let the current flowing in the right most loop be i_1 that is i_1 flows through the capacitor and the load resistor. Let the current flowing through the middle loop be i_2. Also r represents the total resistance in the inductor branch and is given by

$$r = Dr_{DS} + (1 - D)R_F + r_L[5], \tag{2.1}$$

where r_{DS} is the drain to source resistance, R_F is averaged diode resistance and r_L is DC parasitic in inductor.

using Kirchhoff's voltage law, we have

$$(r_C + X_C)(i_2 - i_1) = v_o. \tag{2.2}$$

and

$$-V_I d + (r + X_L)i_1 + v_o = 0, \tag{2.3}$$

Also, the output voltage across the load resistance is given by

$$v_o = \imath_2 R_L. \tag{2.4}$$

From equation (2.3), (2.2) and (2.4),

$$\frac{v_o}{R_L} - \frac{V_I d - v_o}{r + X_L} = \frac{v_o}{r_C + X_C}. \tag{2.5}$$

Manipulating equation (2.5), we have

$$\frac{V_I d}{r + X_L} = v_o \left(\frac{1}{r + X_L} + \frac{1}{R_L} + \frac{1}{r_C + X_L} \right). \tag{2.6}$$

Taking the ratio $\frac{v_o}{d}$ on the left hand side of the equation and remaining onto the right hand side, we get

$$\frac{v_o}{d} = \frac{V_I}{r + X_L} \left(\frac{1}{\frac{1}{r + X_L} + \frac{1}{R_L} + \frac{1}{r_C + X_C}} \right). \tag{2.7}$$

In equation (2.7), the X_L is a complex inductance and is given by sL and X_C represents complex capacitance and is given by $\frac{1}{sC}$ where $s = j\omega$. Therefore the transfer function in S domain can be written as

$$\frac{v_o}{d} = \frac{V_I}{r + sL} \left(\frac{1}{\frac{1}{r + sL} + \frac{1}{R_L} + \frac{1}{\frac{1}{sC} + r_C}} \right). \tag{2.8}$$

Rearranging the equation (2.8) gives us

$$\frac{v_o}{d} = \left(\frac{V_I R_L r_C}{L r_C + R_L L} \right) \frac{s + \frac{1}{r_C C}}{s^2 + s\frac{[C(R_L r_C + R_L r + r r_C) + L]}{LC(R_L + r_C)} + \frac{r + R_L}{LC(R_L + r_C)}}. \tag{2.9}$$

A general representation of the control-to-output transfer function is

$$T_p = T_{px} \frac{s - \omega_{zn}}{s^2 + 2\xi\omega_o s + \omega_o^2}, \tag{2.10}$$

where

$$\omega_{zn} = \frac{1}{r_C C}, \tag{2.11}$$

is the angular frequency of left hand plane zero. The angular corner frequency or the angular undamped natural frequency is given by

$$\omega_o = \sqrt{\frac{r + R_L}{LC(R_L + r_C)}}. \tag{2.12}$$

The damping ratio is given by,

$$\xi = \frac{C[R_L(r_C + r) + r r_C] + L}{2\sqrt{LC(R_L + r_C)(r + R_L)}}. \tag{2.13}$$

The conjugate complex pole is given by

$$p_1, p_2 = -\xi\omega_o \pm \omega_o\sqrt{\xi^2 - 1} = -\xi\omega_o \pm j\omega_o\sqrt{1 - \xi^2}. \tag{2.14}$$

2.4 Open-Loop Control-to-Inductor Current Transfer Function

An open-loop control-to-inductor current transfer function provides a relation that defines any changes in inductor current due to changes in the duty cycle. The small-signal model of the buck converter is shown in Figure 2.3, which can be used to derive this transfer function and relate the inductor current to the control voltage.

Using Kirchhoff's voltage law, gives us

$$V_I d = r i_l + sL i_l + Z_1 i_l \tag{2.15}$$

and

$$V_I = \frac{i_l}{d}[r + sL + Z_1], \tag{2.16}$$

where from Figure 2.3,

$$Z_1 = \frac{1}{\frac{1}{R_L} + \frac{1}{\frac{1}{sC} + r_C}}. \tag{2.17}$$

Substituting equation (2.17) into equation (2.16), we have

$$\frac{i_l}{d} = \frac{V_I}{r + sL + \frac{1}{\frac{1}{R_L} + \frac{1}{\frac{1}{sC} + r_C}}}, \tag{2.18}$$

$$\frac{i_l}{d} = \frac{V_I}{r + sL + \frac{1}{\frac{1}{R_L} + \frac{sC}{sr_CC + 1}}}, \tag{2.19}$$

$$\frac{i_l}{d} = \frac{V_I}{r + sL + \frac{1}{\frac{(sr_CC + 1)R_L}{sr_CC + sR_LC + 1}}}, \tag{2.20}$$

$$\frac{i_l}{d} = \frac{V_I[sr_CC + sR_LC + 1]}{srr_CC + sR_LCr + r + s^2r_CLC + s^2R_LLC + sL + sR_Lr_CC + R_L}, \tag{2.21}$$

$$\frac{i_l}{d} = \frac{V_I[s(r_C C + R_L C) + 1]}{s^2(r_C LC + R_L LC) + s(rr_C C + R_L Cr + L + R_L r_C C) + R_L + r}, \tag{2.22}$$

$$\frac{i_l}{d} = \frac{V_I C(r_C + R_L)}{CL(r_C + R_L)} \frac{s + \dfrac{1}{C(r_C + R_L)}}{s^2 + \dfrac{(rr_C C + R_L Cr + L + R_L r_C C)}{LC(r_C + R_L)} s + \dfrac{R_L + r}{LC(r_C + R_L)}}, \tag{2.23}$$

$$T_i(s) = \frac{i_l}{d} = \frac{V_I}{L} \frac{s + \dfrac{1}{C(r_C + R_L)}}{s^2 + \dfrac{C[rr_C + R_L r + R_L r_C] + L}{LC(r_C + R_L)} s + \dfrac{R_L + r}{LC(r_C + R_L)}} \tag{2.24}$$

is the control-to-inductor current transfer function. A general representation is given by

$$T_i(s) = \frac{i_l}{d} = T_{ix} \frac{s + \omega_{zi}}{s^2 + 2\xi\omega_o + \omega_o^2}, \tag{2.25}$$

$$T_{ix} = \frac{V_I}{L}. \tag{2.26}$$

The DC gain of the transfer function is given by

$$T_{io} = T_i(0) = \frac{V_I}{L} \frac{\omega_{zi}}{\omega_o^2}. \tag{2.27}$$

The left hand plane zero is given by

$$\omega_{zi} = \frac{1}{C(r_C + R_L)}. \tag{2.28}$$

The angular corner frequency or the angular undamped natural frequency is given by

$$\omega_o = \sqrt{\frac{r + R_L}{LC(R_L + r_C)}}. \tag{2.29}$$

The damping ratio is given by

$$\xi = \frac{C(R_L(r_C + r) + rr_C) + L}{2\sqrt{LC(R_L + r_C)(r + R_L)}}. \tag{2.30}$$

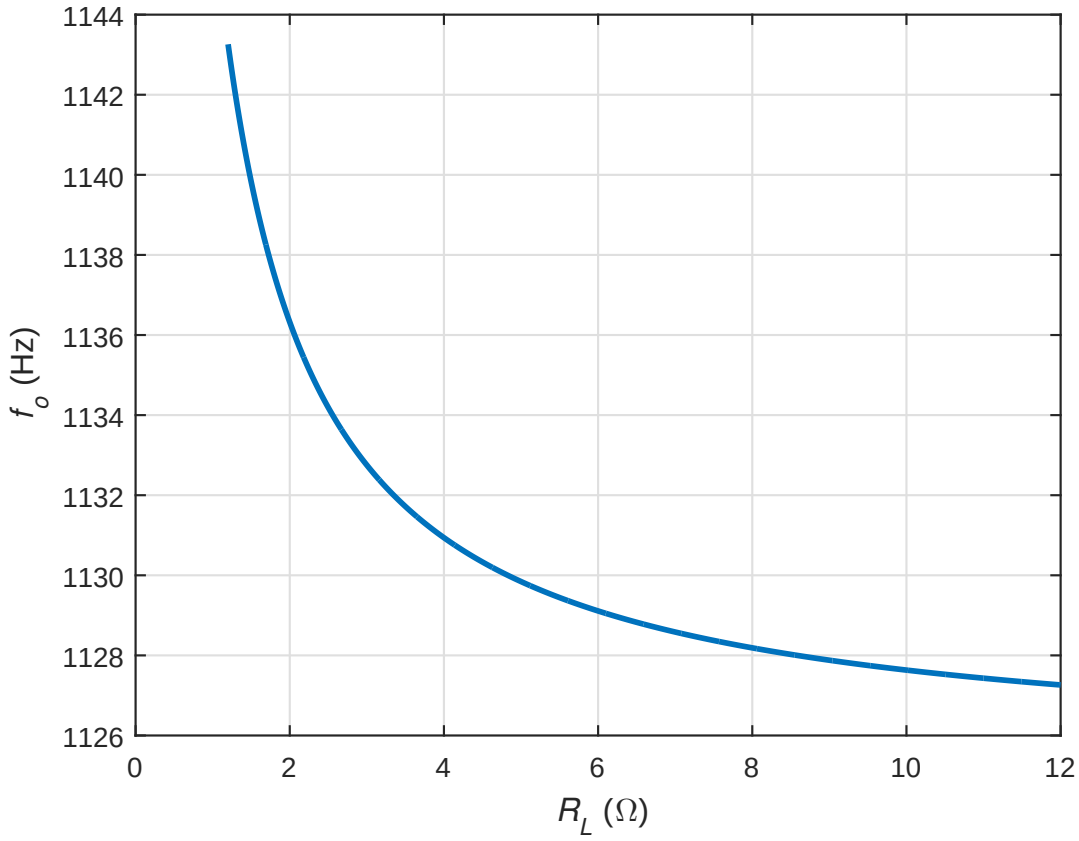

Figure 2.4: Corner frequency as a function of load resistance

The variation of corner frequency f_o and damping coefficient ξ with respect to change in load resistance can be seen in figure 2.4 and 2.5 respectively. the quality factor Q is given by

$$Q = \frac{1}{2\xi}, \tag{2.31}$$

the conjugate complex poles are given by

$$p_1, p_2 = -\xi\omega_o \pm \omega_o\sqrt{\xi^2 - 1} = -\xi\omega_o \pm j\omega_o\sqrt{1 - \xi^2}. \tag{2.32}$$

Substituting $s = j\omega$ into (2.25) yields

$$T_i(j\omega) = T_{io}\frac{\left(1 + \frac{j\omega}{\omega_{zi}}\right)}{1 + \left(\frac{\omega}{\omega_o}\right)^2 + 2j\xi\left(\frac{\omega}{\omega_o}\right)} = |T_i|e^{j\phi_{T_i}}, \tag{2.33}$$

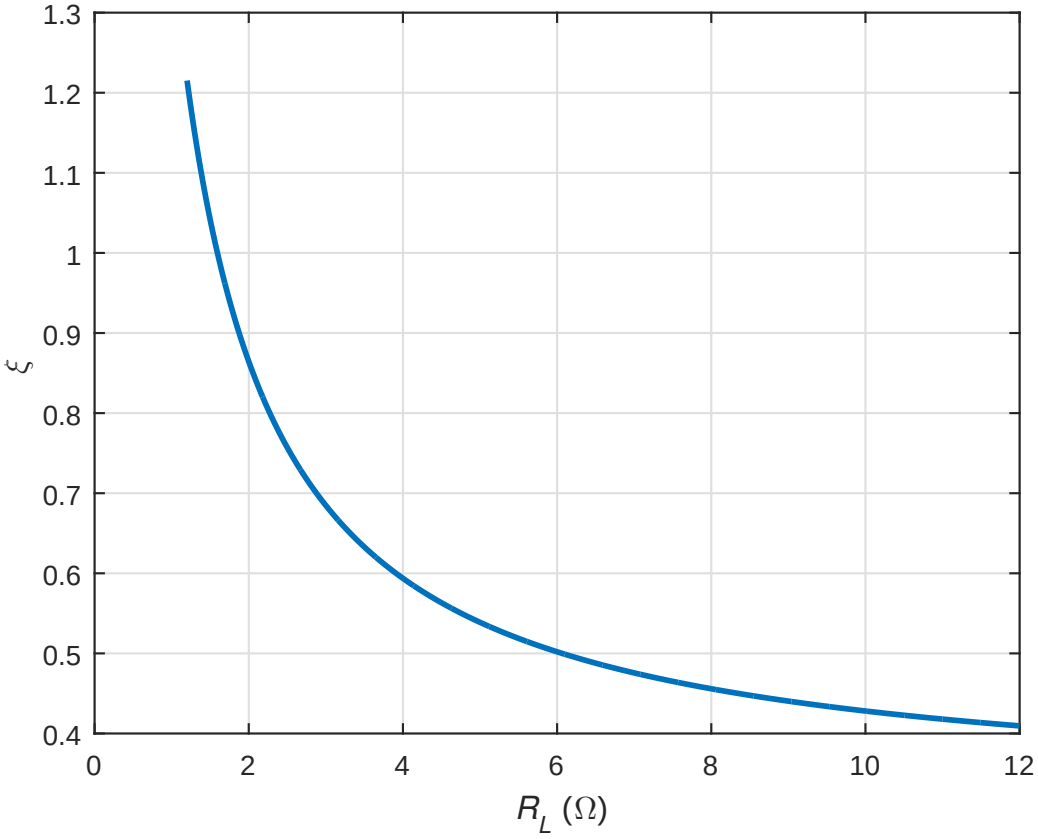

Figure 2.5: Damping factor as a function of load resistance

where

$$|T_i| = T_{io}\sqrt{\frac{1+\left(\frac{\omega}{\omega_{zi}}\right)^2}{\left[1-\left(\frac{\omega}{\omega_o}\right)^2\right]^2+4\xi^2\left(\frac{\omega}{\omega_o}\right)}} \tag{2.34}$$

and

$$\phi_{T_i} = \arctan\left(\frac{\omega}{\omega_{zi}}\right) - \arctan\left[\frac{2\xi\left(\frac{\omega}{\omega_o}\right)}{1-\left(\frac{\omega}{\omega_o}\right)^2}\right], \text{ for } \frac{\omega}{\omega_o} \leq 1. \tag{2.35}$$

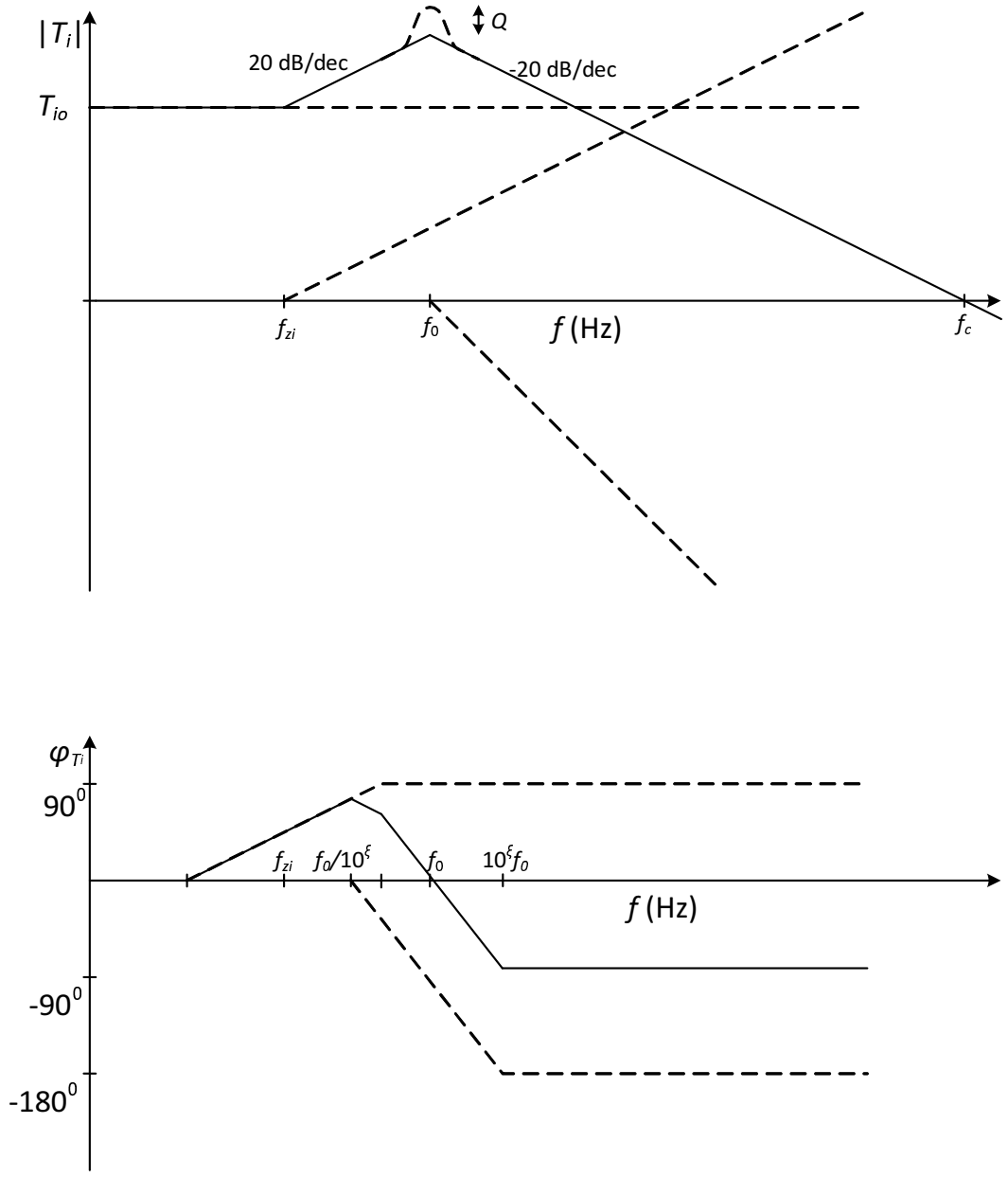

Figure 2.6: Idealized Bode plots of the open-loop control-to-inductor current transfer function T_i for the buck converter

The asymptotic bode plot can be seen in Figure 2.6. It is to be noted that the figure represents an ideal version of the magnitude and frequency response. But due to the presence of conjugate complex poles there will be a peak in the magnitude plot. For high values of damping coefficient ξ the peak is lower and vice versa. This

peak can be denoted by the quality factor as given in equation 2.31

2.5 Open-Loop Input-to-Output Voltage Transfer Function

The input-to-output voltage transfer function, also known as the audio susceptibility of the system can be obtained by setting $d = 0$ and $i_o = 0$ in Figure 2.2 to obtain a small-signal model as shown in Figure 2.7.

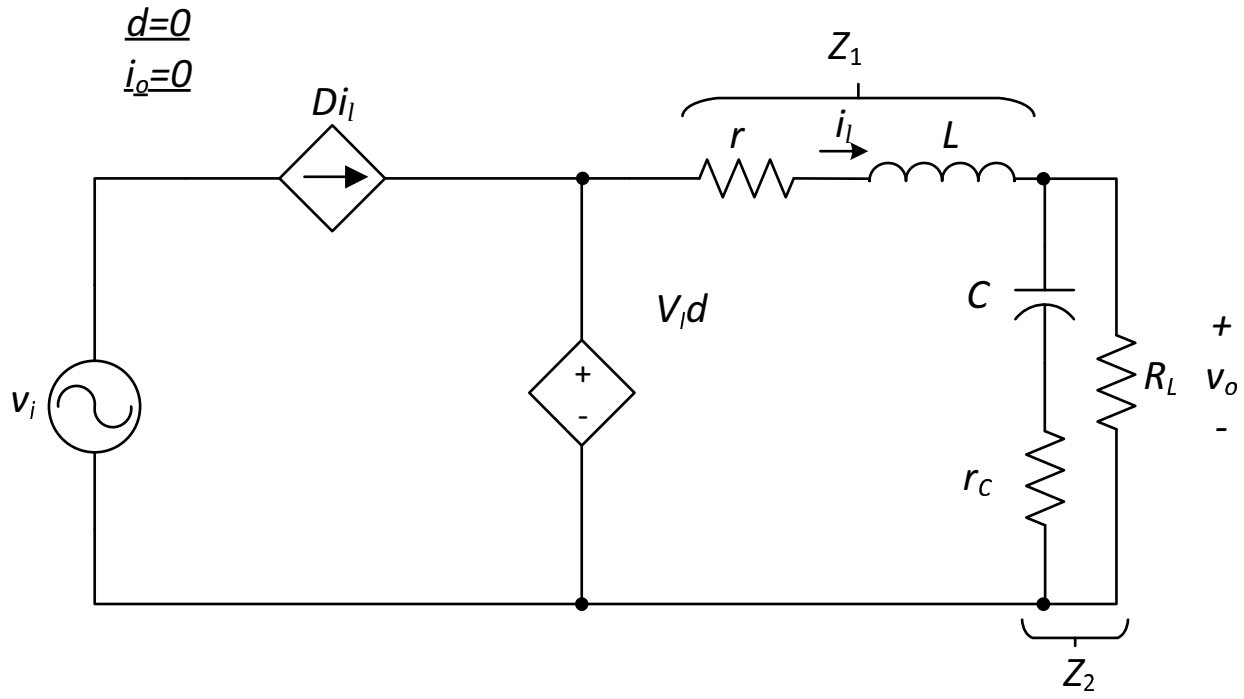

Figure 2.7: Small-signal model of a buck DC-DC converter to derive input-to-output voltage transfer function

Using Kirchhoff's voltage law in second loop gives us,

$$i_l(r + X_L) + (X_C + r_C)(i_l - i_o) - Dv_i = 0. \tag{2.36}$$

Applying Kirchhoff's voltage law in the right most loop gives us,

$$v_o + (i_o - i_l)(X_C + r_C) = 0, \tag{2.37}$$

$$\frac{-v_o}{X_C + r_C} = i_o - i_l, \tag{2.38}$$

$$i_l = i_o + \frac{v_o}{X_C + r_C}. \tag{2.39}$$

The small signal output current is given as

$$i_o = \frac{v_o}{R_L}. \tag{2.40}$$

From equation (2.36) and (2.39)

$$(i_o + \frac{v_o}{X_C + r_C})(r + X_L) + (X_C + r_C)(i_o + \frac{v_o}{X_C + r_C} - i_o) - Dv_i = 0. \tag{2.41}$$

From equation (2.40) and (2.41)

$$i_o(r + X_L) + \frac{v_o}{X_C + r_C}(r + X_L) + v_o - Dv_i = 0, \tag{2.42}$$

$$v_o\left(\frac{r + X_L}{R_L} + \frac{r + X_L}{X_C + r_C} + 1\right) = Dv_i, \tag{2.43}$$

$$\frac{v_o}{v_i} = \frac{D}{\frac{r + X_L}{R_L} + \frac{r + X_L}{X_C + r_C} + 1}, \tag{2.44}$$

$$\frac{v_o}{v_i} = \frac{D(R_L X_C + R_L r_C)}{rX_C + r_C r + R_L r + X_C X_L + r_C X_L + R_L X_C + R_L r_C}, \tag{2.45}$$

$$\frac{v_o}{v_i} = \frac{DR_L\left(\frac{1}{sC} + r_C\right)}{\frac{r}{sC} + r_C r + R_L r + \frac{L}{C} + r_C Ls + R_L Ls + \frac{R_L}{sC} + R_L r_C}, \tag{2.46}$$

$$\frac{v_o}{v_i} = \frac{\frac{DR_L r_C}{s}\left(\frac{1}{Cr_C} + s\right)}{s(r_C L + R_L L) + r_C r + R_L r + \frac{L}{C} + R_L r_C + \frac{r + R_L}{sC}}, \tag{2.47}$$

$$\frac{v_o}{v_i} = \frac{DR_L r_C\left(s + \frac{1}{Cr_C}\right)}{s^2 C[r_C L + R_L L] + [C(r_C r + R_L r + R_L r_C) + L]s + r + R_L}, \tag{2.48}$$

$$M_v = \frac{DR_L r_C}{L(r_C + R_L)} \frac{s + \dfrac{1}{Cr_C}}{s^2 + \dfrac{C[r_C r + R_L(r + r_C)] + L}{CL(r_C + R_L)} s + \dfrac{r + R_L}{LC(r_C + R_L)}}. \tag{2.49}$$

is the input-to-output voltage transfer function of a buck DC-DC converter the general representation of this transfer function is given by

$$M_v = M_{vx} \frac{s - \omega_{zl}}{s^2 + 2\xi\omega_o + \omega_o^2}, \tag{2.50}$$

where

$$M_{vx} = \frac{DR_L r_C}{l(r_C + R_L)}. \tag{2.51}$$

The angular frequency of the left-half plane zero is given by

$$\omega_{zl} = \frac{1}{Cr_C}. \tag{2.52}$$

The angular corner frequency or the angular undamped natural frequency is given by

$$\omega_o = \sqrt{\frac{r + R_L}{LC(R_L + r_C)}}. \tag{2.53}$$

The damping ratio is given by,

$$\xi = \frac{C[R_L(r_C + r) + rr_C] + L}{2\sqrt{LC(R_L + r_C)(r + R_L)}}, \tag{2.54}$$

the conjugate complex pole is given by

$$p_1, p_2 = -\xi\omega_o \pm \omega_o\sqrt{\xi^2 - 1} = -\xi\omega_o \pm j\omega_o\sqrt{1 - \xi^2}. \tag{2.55}$$

2.6 Open-Loop Input Impedance Transfer Function

The open equivalent circuit used in Figure 2.7 can also be used to obtain the input impedance transfer function.

Using Kirchhoff's voltage law,

$$(r + X_L)i_l + v_o - Dv_i = 0, \tag{2.56}$$

$$(r + X_L)i_l + i_l Z_1 - Dv_i = 0, \tag{2.57}$$

where input current is given by $i_i = i_l D$

$$i_i(r + X_L + Z_1) - D^2 v_i = 0, \tag{2.58}$$

$$\frac{v_i}{i_i} = \frac{r + X_L + Z_1}{D^2}, \tag{2.59}$$

$$\frac{v_i}{i_i} = \frac{1}{D^2}\left(r + sL + \frac{\frac{R_L}{sC}}{R_L + \frac{1}{sC} + r_C}\right), \tag{2.60}$$

$$\frac{v_i}{i_i} = \frac{1}{D^2}\left(\frac{rR_L + \frac{r}{sC}rr_C + sLR_L + \frac{L}{C} + sLr_C + \frac{R_L}{sC} + R_L r_C}{R_L + r_C + \frac{1}{sC}}\right), \tag{2.61}$$

$$\frac{v_i}{i_i} = \frac{1}{D^2 C(R_L + r_C)}\left(\frac{r + R_L + sC(rR_L + rr_C + \frac{L}{C}) + s^2 LC(R_L + r_C)}{s + \frac{1}{C(R_L + r_C)}}\right), \tag{2.62}$$

$$\frac{v_i}{i_i} = \frac{L}{D^2}\left[\frac{s^2 + s\frac{C(rr_C + R_L(r + r_C)) + L}{LC(R_L + r_C)} + \frac{r + R_L}{LC(R_L + r_C)}}{s + \frac{1}{C(R_L + r_C)}}\right]. \tag{2.63}$$

The general representation of the this transfer function is given as

$$Z_i = Z_{ix}\frac{s^2 + 2\xi\omega_o s + \omega_o^2}{s - \omega_{rc}}, \tag{2.64}$$

where

$$Z_{ix} = \frac{L}{D^2}. \tag{2.65}$$

The angular frequency of left-half plane pole is given by

$$\omega_{rc} = \frac{1}{C(R_L + r_C)}. \tag{2.66}$$

2.7 Open-Loop Output Impedance Transfer Function

The small-signal model of a buck converter can be reduced by setting d, v_i, and i_o to zero and applying an independent voltage source v_t, which will force current i_l into the system. Now the ratio of v_t by i_t will give us the output impedance of the converter. The small-signal model required for the output impedance can be seen in Figure 2.8. From the Figure the voltage v_t is being applied to the total impedance and therefore can be calculated as

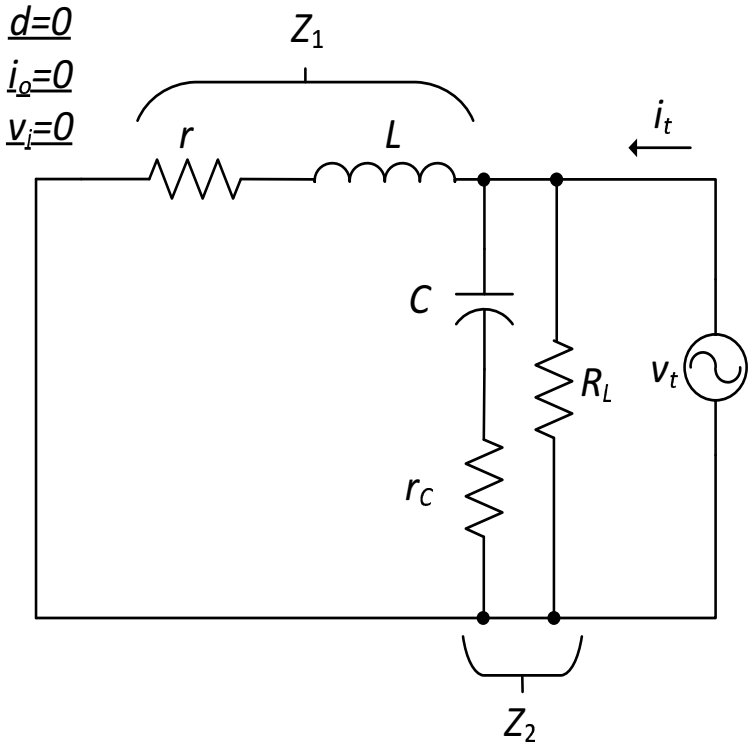

Figure 2.8: Small-signal model of a buck DC-DC converter to derive output impedance

$$v_t = i_t \left[\frac{Z_1(X_L + r)}{Z_1 + X_L + r} \right], \tag{2.67}$$

$$\frac{v_t}{i_t} = \frac{\dfrac{R_L(X_C + r_C)(X_L + r)}{R_L + X_C + r_C}}{\dfrac{R_L(X_C + r_C)}{R_L + X_C + r_C} + X_L + r}, \tag{2.68}$$

$$\frac{v_t}{i_t} = \frac{R_L(X_C + r_C)(X_L + r)}{R_L(X_C + r_C) + (X_L + r)(R_L + X_C + r_C)}, \tag{2.69}$$

$$\frac{v_t}{i_t} = \frac{R_L\left(\dfrac{1}{sC} + r_C\right)(sL + r)}{\dfrac{R_L}{sC} + r_C R_L + sR_L L + \dfrac{L}{C} + sr_C L + rR_L + \dfrac{r}{sC} + rr_C}, \tag{2.70}$$

$$\frac{v_t}{i_t} = R_L C r_C L \frac{\left(s + \dfrac{1}{CrC}\right)\left(s + \dfrac{r}{L}\right)}{s^2 C(r_C L + R_L L) + (R_L r_C + \dfrac{L}{C} + rR_L + rr_C)sC + r + R_L}, \tag{2.71}$$

$$Z_o = \frac{R_L r_C}{r_C + R_L} \frac{\left(s + \dfrac{1}{Cr_C}\right)\left(s + \dfrac{r}{L}\right)}{s^2 + \dfrac{C[r_C r + R_L(r + r_C)] + L}{CL(r_C + R_L)} s + \dfrac{r + R_L}{LC(r_C + R_L)}} \tag{2.72}$$

is the output impedance of the buck converter. The general representation of this transfer function is given by

$$Z_o = Z_{ox} \frac{(s - \omega_{zl})(s - \omega_{zm})}{s^2 + 2\xi\omega_o s + \omega_o^2}, \tag{2.73}$$

where

$$Z_{ox} = \frac{R_L r_C}{r_C + R_L}. \tag{2.74}$$

The angular frequency of left-half plane zeros are given by

$$\omega_{zl} = \frac{1}{Cr_C} \tag{2.75}$$

and

$$\omega_{zm} = \frac{r}{L}. \tag{2.76}$$

The angular corner frequency or the angular undamped natural frequency is given by

$$\omega_o = \sqrt{\frac{r + R_L}{LC(R_L + r_C)}}. \tag{2.77}$$

The damping ratio is given by,

$$\xi = \frac{C[R_L(r_C + r) + rr_C] + L}{2\sqrt{LC(R_L + r_C)(r + R_L)}}. \tag{2.78}$$

The conjugate complex poles is given by

$$p_1, p_2 = -\xi\omega_o \pm \omega_o\sqrt{\xi^2 - 1} = -\xi\omega_o \pm j\omega_o\sqrt{1 - \xi^2}. \tag{2.79}$$

Knowing these transfer functions helps analyze the open-loop system response of a system. These responses can be altered by using controllers. In this thesis, controllers will be designed to sense and control the inductor current and the output voltage. Types of controllers and their functions will be briefed in the next chapter.

3 Controllers

3.1 Introduction

There are many specific objectives that any general system tries to accomplish. For instance, an air conditioner tries to regulate constant room temperature, speed of an automobile is to be maintained depending upon the amount of acceleration provided by the driver. To accomplish such objectives requires a use of certain control systems. A control system senses for the signal, which is to be controlled and provides required compensation such that the system always successfully fulfills its task [6]. Depending on the type of signal the controller senses, there are different types of controllers available for example, a voltage-mode controller or a current-mode controller. Since the objective of this thesis is to control a buck DC-DC converter, the signals sensed in this system are voltage and current. Thus, voltage and a current-mode control will be utilized.

3.2 Voltage-Mode Control

A voltage-mode controller senses voltage and compares it to a reference voltage to obtain an error voltage. Depending on error voltage the controller decides the compensation it should provide to regulate the sensed voltage. There are many types of conventional voltage-mode controllers like a proportional controller, in which the sensed voltage is multiplied by a constant, An integral controller, which adds an extra pole to the transfer function or a derivative controller, which added a zero to the transfer function. These controllers along with their combination can be used to help shape the sensed voltage. This includes reducing settling time, rise time, overshoots and undershoots.

A general representation of a voltage-mode controller can be seen in Figure 3.1. The transfer function of such a controller is given by the equation (3.1). Now depending

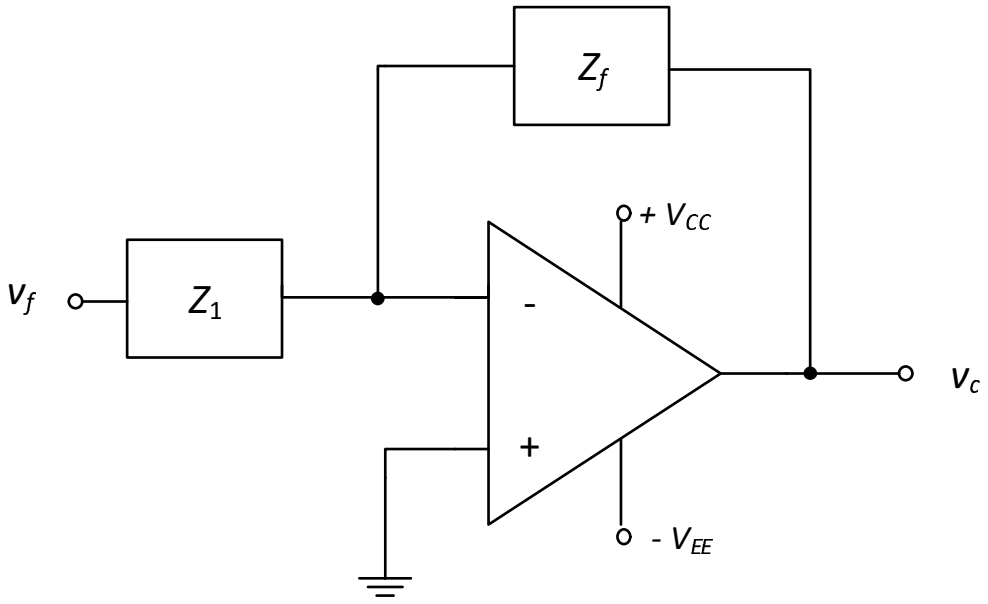

Figure 3.1: Block diagram of an op-amp as a controller

on the selection of passive components for Z_1 and Z_f the controller shown in Figure 3.1 can behave as a proportion or integral or differencial controller or even the combination of the three. Each of these controllers are described in brief as follow

$$\frac{v_c}{v_f} = -\frac{Z_f}{Z_1} \tag{3.1}$$

3.2.1 Proportional Controller

Using a pure resistive Z_1 and Z_f , the input-to-output transfer function of the controller is independent of the frequency and thus output of such a controller is amplified. The transfer function of such an amplifier is given in equation (3.2). Figure 3.2 represents a proportional amplifier.

$$\frac{v_c}{v_f} = -\frac{R_f}{R_1} \tag{3.2}$$

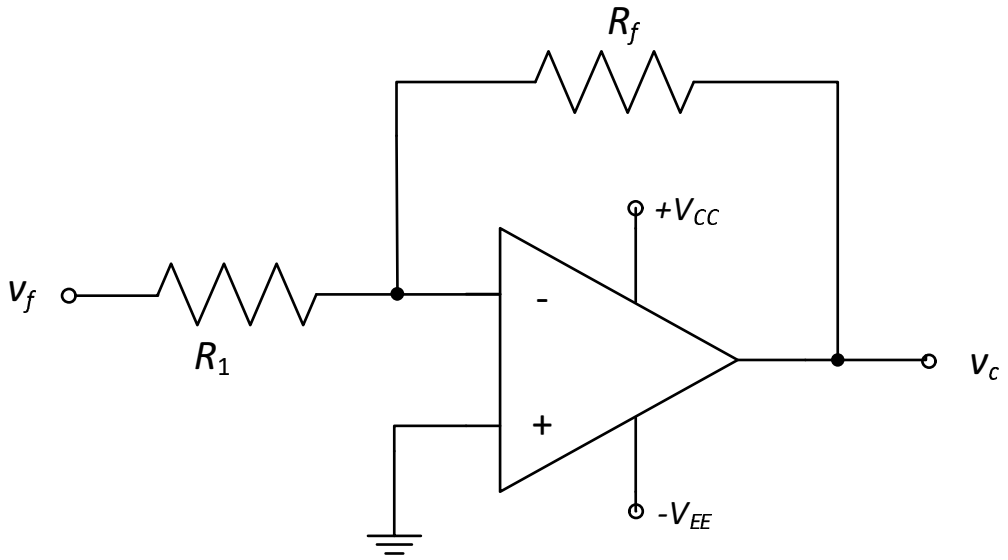

Figure 3.2: Circuit diagram of a proportional controller

3.2.2 Differentiator

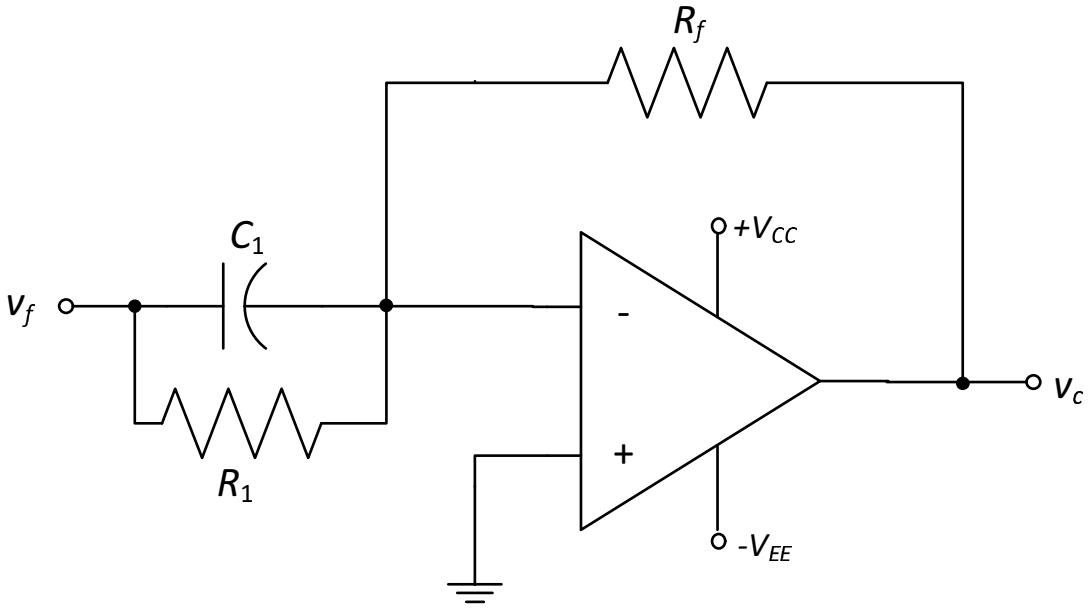

Figure 3.3: Circuit diagram of a differentiator

Using an inductor in feedback loop of the controller or using a capacitor in place of Z_1 adds a zero in its transfer function. Hence any input provided to such an

op-amp gets differentiated and is obtained in the output. Such a controller is very sensitive because of the inductive nature and therefore are usually susceptible to noises. The voltage input to output transfer function of such a differenciator is as shown in equation (3.3). Figure 3.3 represents a differentiator.

$$\frac{v_c}{v_f} = -R_f C_1 \left(s + \frac{1}{C_1 R_1} \right) \tag{3.3}$$

3.2.3 Integrator

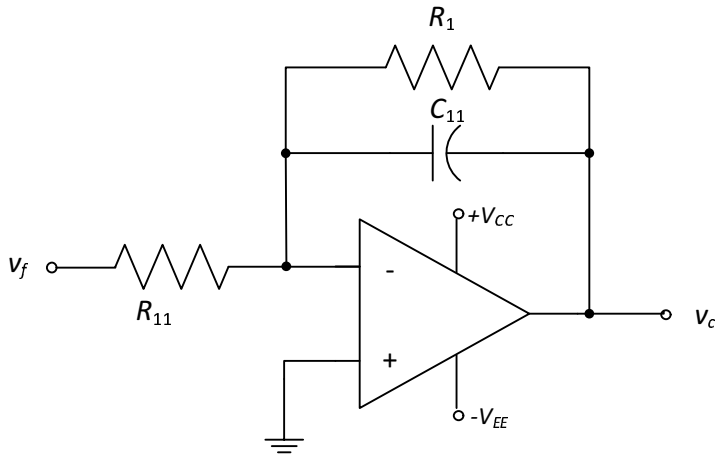

Figure 3.4: Circuit diagram of an integrator

An op-amp can be used as an integrator by using a capacitor in its feedback loop, which creates a pole in its transfer function, doing so for the high frequencies averages out the input to the op-amp. An example to an op-amp acting as an integrator can be seen in Figure 3.4. Here adding a resistance in parallel to the capacitance makes sure that the feedback of the op-amp does not turn into an open circuit, when the capacitor discharges and hence helps in maintaining a stable feedback system. The input to output transfer function of such an op-amp is given by the equation (3.4). Also using such a controller adds a pole to the loop gain of the system, which helps in reducing the steady state error to zero and also reduce the settling time but sometimes

is also responsible for overshoots.

$$\frac{v_c}{v_f} = -\frac{1}{R_{11}C_{11}}\left(\frac{1}{s+\frac{1}{C_{11}R_1}}\right) \tag{3.4}$$

3.3 Current-Mode Control

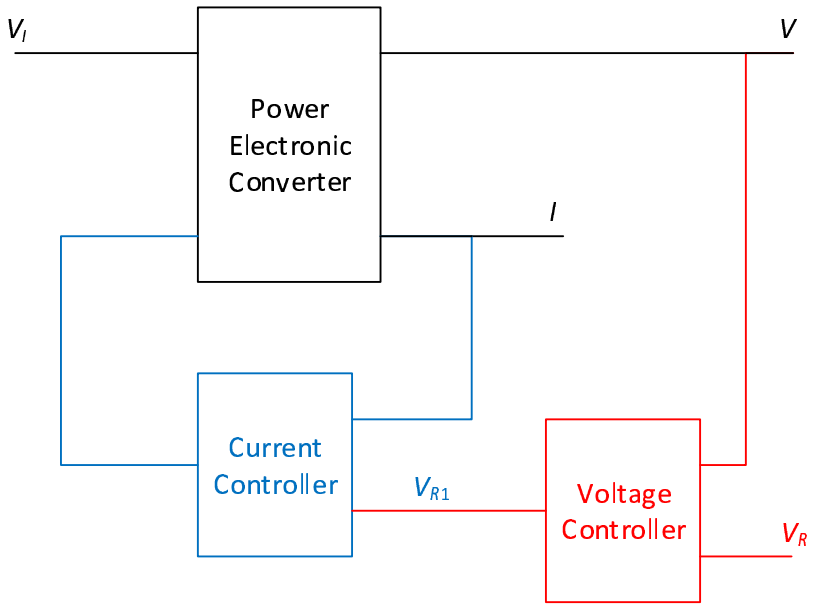

Figure 3.5: Block Diagram representing a general current control scheme

A current-mode controller first senses a current signal and converts it into voltage by using a sense resistance. Now, this sensed current is compared to a reference voltage provided to the controller to obtain an error signal. Depending on the magnitude of the error signal the current-mode controller provides the required compensation to control the sensed current. A current-mode controller provides a higher order of control, when compared to a voltage-mode control. In many cases a current-mode controller is usually integrated along with a voltage-mode controller. A general representation of one such control scheme is as shown in Figure 3.5, which represents an inner current loop and an outer voltage loop. The inner loop helps control the current signal depending on the reference voltage that has been provided by the control signal

of the outer voltage loop. The outer voltage control loop controls the voltage signal depending on the reference voltage that has been provided to the voltage controller. Depending on the property of the current signal that the controller tries to manipulate, there are different types of current-mode controllers like, a peak current-mode controller, valley current-mode controller or an average current-mode controller. A peak current-mode controller is the most common controller used for controlling a current signal for a power electronic converter but has a few drawbacks like, false triggering due to harmonics in the system and no control over controller gain. A first order, type one average current-mode controller is introduced as its replacement.

3.3.1 Peak Current-Mode Control

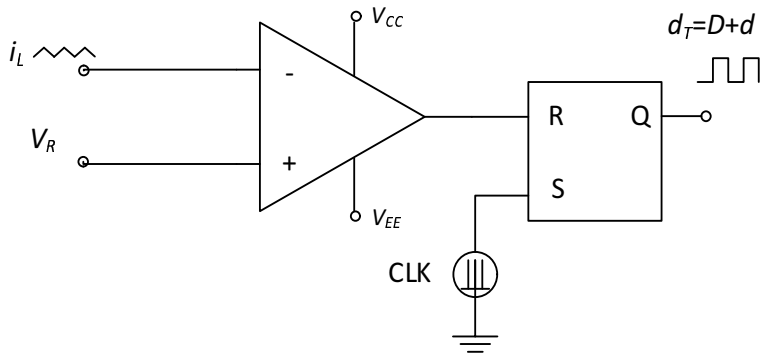

Figure 3.6: Circuit diagram of a peak current-mode controller[5]

A peak current-mode controller without slope compensation is connected as shown in Figure 3.6. Since the on time of a buck converter decides the peak value of the inductor current a variable duty cycle can be used as a control signal. In this type of current-mode control, the non-inverting terminal of the op-amp is connected to a reference voltage and the current, which is to be controlled is sensed and converted to voltage by using a sense resistance and is connected to the inverting terminal. Here the op-amp acts as a comparator. Whenever, the sensed voltage reaches the reference voltage, the op-amp saturates to V_{EE}. Thus, giving low signal to the reset of the

latch. These signals along with the clock produces duty cycle for MOSFET. This duty cycle drives the DC-DC power electronic buck converter. Any rise in the peak value of the inductor current will be prevented by this controller by switching the MOSFET off.

3.3.2 Average Current-Mode Control

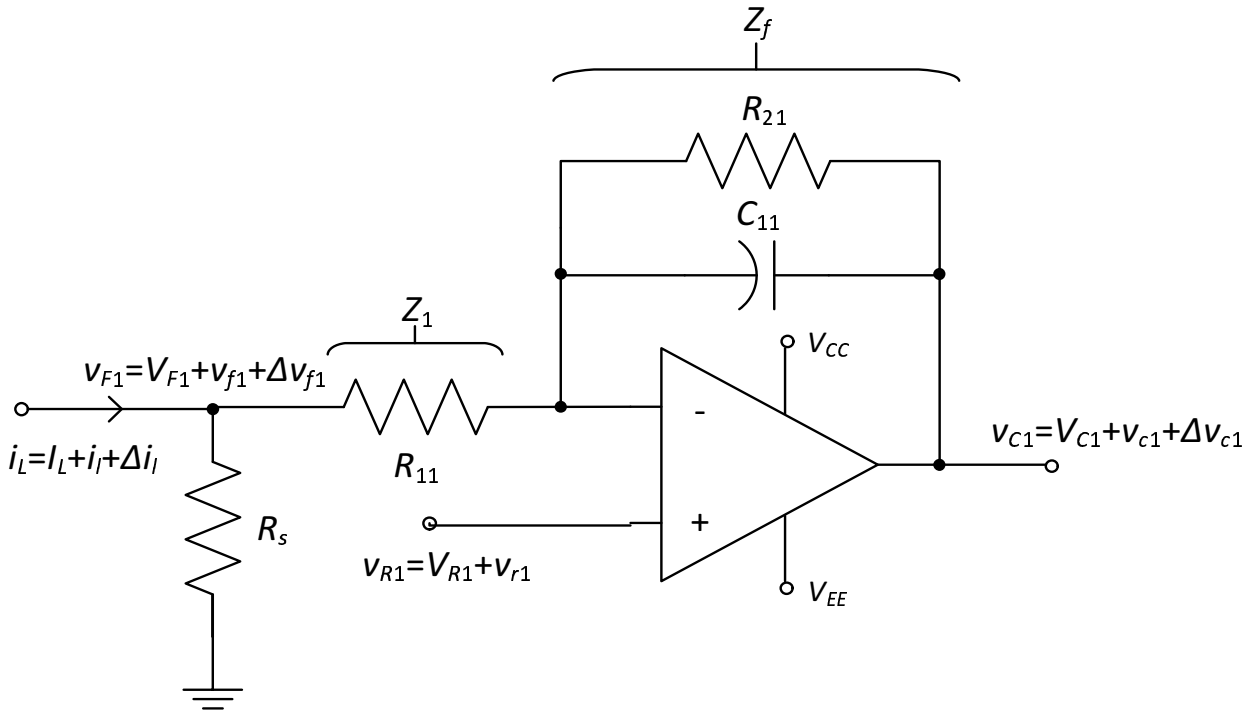

Figure 3.7: Circuit diagram of an average current-mode control

An average current-mode controller is connected as shown in Figure 3.7. It compares an average value of the sensed voltage to a reference voltage v_{R1} to generate error voltage v_{E1}. Depending on this error voltage required, compensation is needed. This controller can be implemented onto a buck converter to control its inductor current. Here, the inductor current is the sensed current. Since, an op-amp can compare only voltages, the inductor current is converted into a voltage by using a sense resistor R_s. The voltage across this resistor can now be called sense voltage v_{F1}, which is then compared to V_{R1}.

The inductor current has three main components namely, average DC current I_L, the AC ripples due to switching Δi_l and small signal perturbation i_l. All three components are sensed to get their respective voltage equivalents V_{F1}, Δv_{f1} and v_{f1} respectively as shown in Figure 3.7. The current profile without the perturbations can be seen in Figure 3.8. The inductor current can be represented as

$$i_L = I_L + \Delta i_l + i_l. \tag{3.5}$$

This inductor current is sensed and is converted into voltage by using a sense resistance

$$v_{F1} = R_s i_L. \tag{3.6}$$

This sensed feedback voltage will also have the components of the inductor current.

$$v_{F1} = V_{F1} + \Delta v_{f1} + v_{f1}. \tag{3.7}$$

The reference voltage of this controller has a DC component V_{R1} but if this voltage is sensed from the outer voltage feedback loop it may contain small signal perturbations given by v_{r1} given by

$$v_{R1} = V_{R1} + v_{r1}. \tag{3.8}$$

The error voltage is the difference between the feedback voltage and the reference voltage

$$v_{E1} = v_{R1} - v_{F1}, \tag{3.9}$$

from equation (3.7), (3.8) and (3.9)

$$v_{E1} = V_{R1} - V_{F1} + v_{r1} - v_{f1} - \Delta v_{f1}. \tag{3.10}$$

The control voltage of the controller is given by

$$v_{C1} = v_{R1} + \frac{Z_f}{Z_i} v_{E1}, \tag{3.11}$$

from equation 3.8 and 3.11

$$v_{C1} = V_{R1} + v_{r1} + \frac{Z_f}{Z_i}(V_{R1} - V_{F1} + v_{r1} - v_{f1} - \Delta v_{f1}). \tag{3.12}$$

Therefore, the control voltage also has three components namely a DC control voltage V_{C1} given by

$$V_{C1} = V_{R1}\frac{Z_f(0)}{Z_i(0)}(V_{R1} - V_{F1}). \tag{3.13}$$

The control voltage due to small signal perturbations

$$v_{c1} = v_{r1} + \frac{Z_f(s)}{Z_i(s)}(v_{r1} - v_{f1}), \tag{3.14}$$

and the third components in the control voltage is due to the ripples present in the inductor current given by

$$\Delta v_{c1} = -\frac{Z_f(s)}{Z_i(s)}(\Delta v_{f1}). \tag{3.15}$$

It should be noted that if a constant voltage source V_{R1} is used as a reference voltage, a small signal disturbance v_{r1} can be set to zero simplifying 3.14 to

$$v_{c1} = -\frac{Z_f(s)}{Z_i(s)}(v_{f1}). \tag{3.16}$$

It is to be noted from equation (3.13) that if a controller with a constant non-time varying gain is used the control voltage will resemble the waveform as shown in Figure 3.8(b), which is an amplified or an attenuated version of the sensed inductor current depending on the controller gain. Also, it is to be noted that since an inverting op-amp is used, the control voltage has a phase difference of 180^0 with respect to sensed inductor current. From equation (3.15), since the gain is no longer constant and varies with frequency, the control voltage v_{c1} has ripples as a function of $\frac{Z_f(s)}{Z_i(s)}$, which is a function of frequency. The controller with a magnitude plot as shown in Figure 3.11 will have a high gain at low frequencies and after the crossover frequency of the controller, it will attenuate the sensed signal. A controller with such a magnitude plot can be obtained by using a capacitor in Z_f. Now, for a first order type one controller

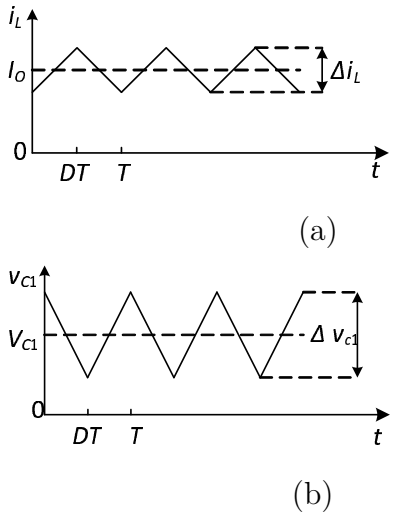

Figure 3.8: (a) Waveform of inductor current of a buck DC-DC converter. (b) Waveform of control voltage of a pulse-width modulator which is an amplified version of the sensed inductor current.

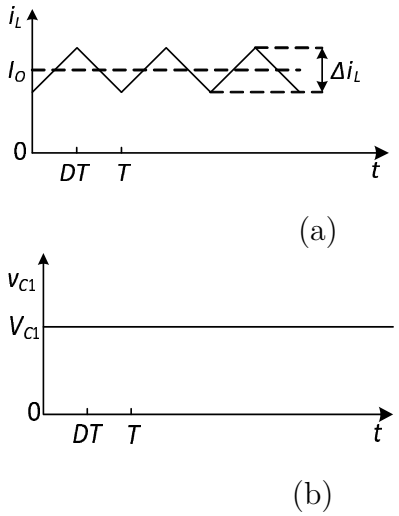

Figure 3.9: (a) Waveform of inductor current of a buck DC-DC converter. (b) Waveform of control voltage of a pulse-width modulator when cross over frequency of the controller is less than the switching frequency of the buck DC-DC converter.

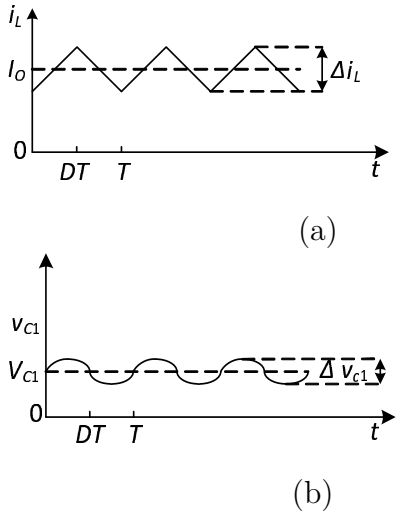

Figure 3.10: (a) Waveform of inductor current of a buck DC-DC converter. (b) Waveform of control voltage of a pulse-width modulator when cross over frequency of the controller is higher than the switching frequency of the buck DC-DC converter.

as shown in Figure 3.7, the cross over frequency is given by $f_C = \dfrac{1}{2\pi R_{21} C_{11}}$. Since the ripples in inductor current due to switching oscillate at switching frequency of the buck converter, a controller designed with a cross over frequency less than the switching frequency of the converter will attenuate these ripples and produce a pure DC control voltage given by equation (3.13) and as shown in Figure 3.9(b). Now, this control signal is sent to an analog-to-digital converter, which compares this control voltage to a triangular reference voltage to generate pluses as shown in Figure 3.12

If the controller's cross over frequency is more than the switching frequency of the buck converter then the control voltage will have small components of the ripple voltage present in it as a function of frequency represented by equation (3.15). The obtained waveform can be seen in Figure 3.10(b) and due to the capacitive nature the control voltage will lag behind the sensed voltage. Therefore the control voltage will have certain phase difference with sensed voltage. But the controller still can be used to control the buck DC-DC converter. The waveform of the control voltage with the triangular reference voltage can be seen in Figure 3.13

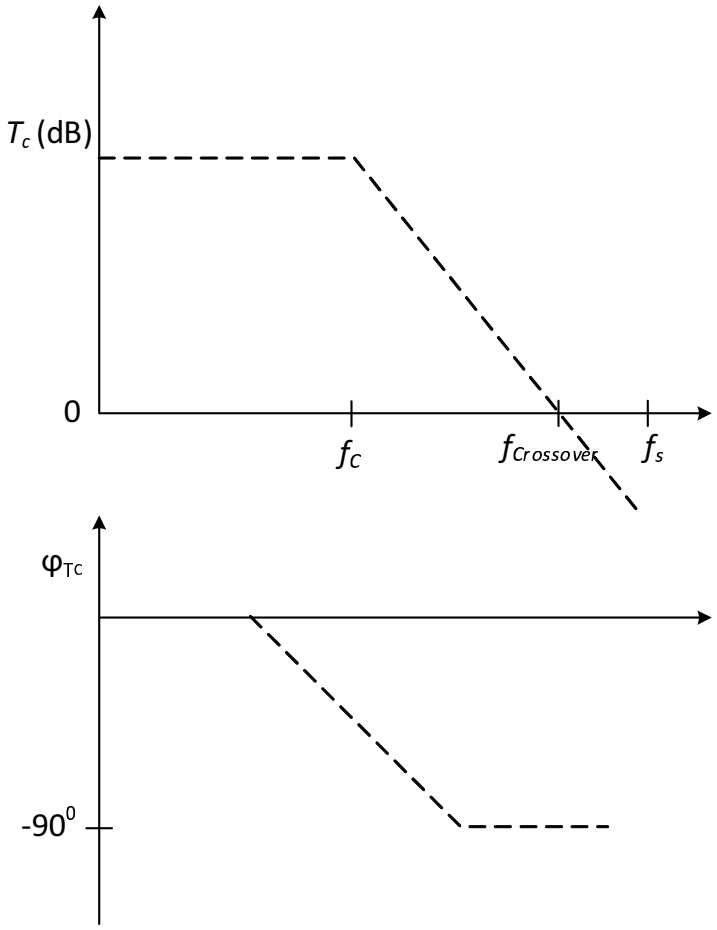

Figure 3.11: Magnitude and phase plot of a first order type one average current-mode controller

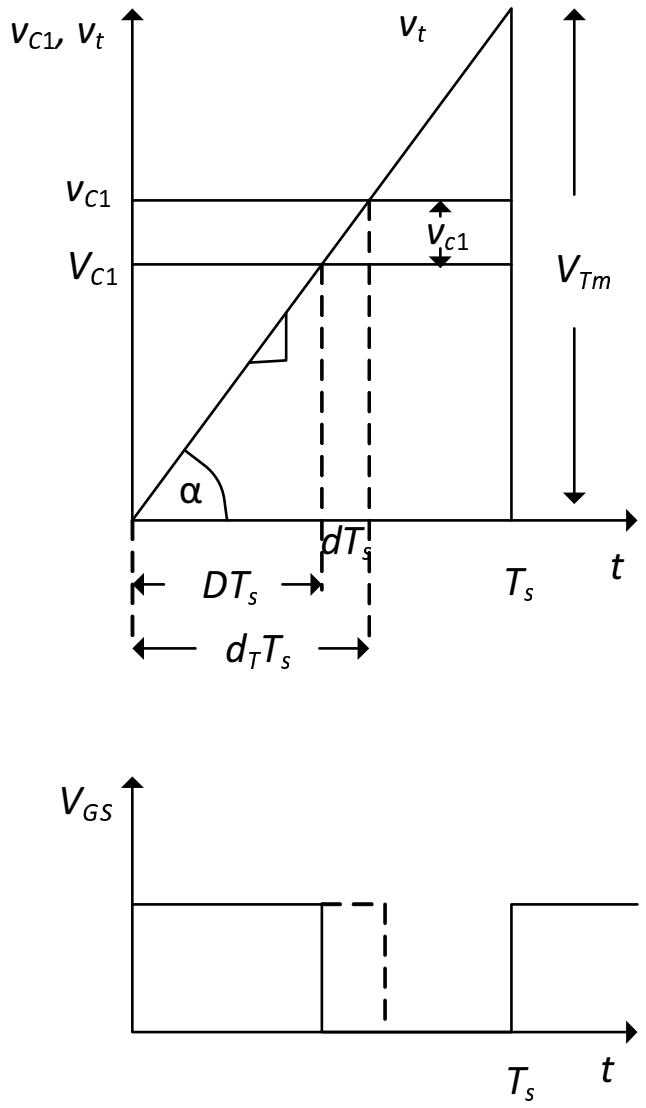

Figure 3.12: Waveforms in the pulse-width modulator representing the sawtooth voltage v_t, the control voltage v_{C1} and gate-to-source voltage v_{GS} for controller crossover frequency less than the switching frequency.[5]

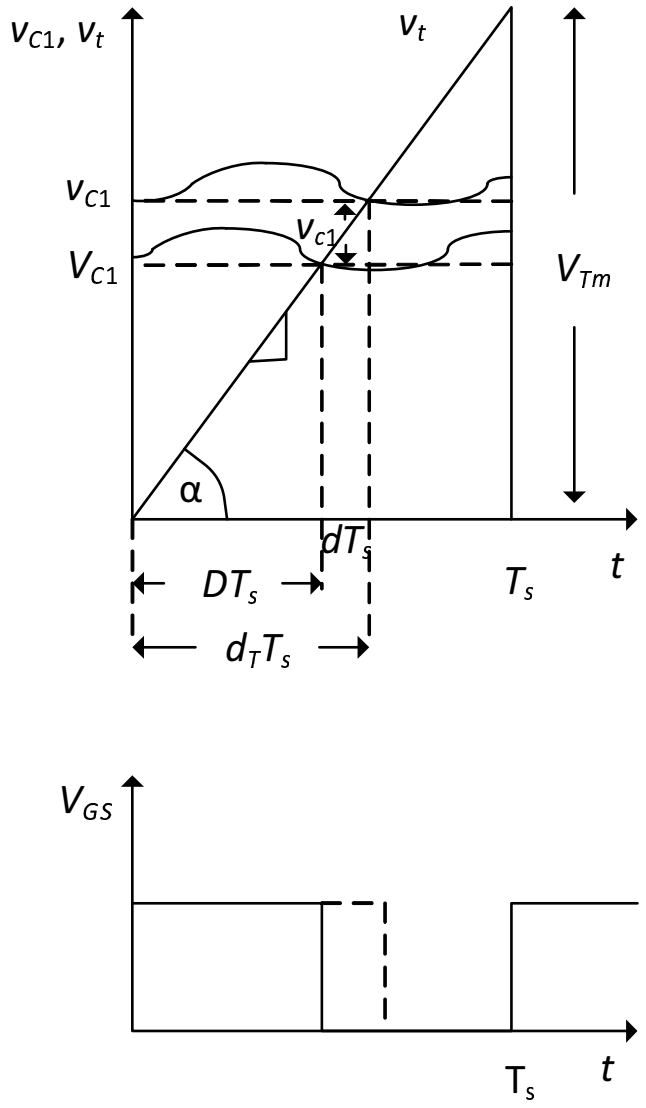

Figure 3.13: Waveforms in the pulse-width modulator representing the sawtooth voltage v_t, the control voltage v_{C1} and gate-to-source voltage v_{GS} for controller crossover frequency more than the switching frequency.

4 Design

4.1 Introduction

This chapter provides all the design procedures one needs to follow to obtain a controlled buck DC-DC converter using a first order average current-mode controller. All the required plots to support the design are plotted for analysis. The design procedure is going to start off by designing a buck DC-DC converter. Based on the compensation it requires a current-mode controller to control the inductor current and a voltage-mode controller to control the output voltage will be designed and implemented.

4.2 Design of an Open-Loop Buck DC-DC Converter in Continuous Conduction Mode

A buck converter is designed[5] for the following specifications:
$V_I = 28 \pm 4$ V, $V_O = 12$ V, $I_{Omin} = 1$ A, $I_{Omax} = 10$ A $f_s = 100$ kHz. This same design will be used for the rest of this thesis and will be the basis for designing the controllers.
From the given specifications minimum and maximum power offered by the converter are

$$P_{Omin} = V_O I_{Omin} = 12 \times 1 = 12 \text{ W} \tag{4.1}$$

and

$$P_{Omax} = V_O I_{Omax} = 12 \times 10 = 120 \text{ W}. \tag{4.2}$$

The minimum, maximum and nominal values of load resistance are given by

$$R_{Lmin} = \frac{V_O}{I_{Omax}} = \frac{12}{10} = 1.2 \ \Omega, \tag{4.3}$$

$$R_{Lmax} = \frac{V_O}{I_{Omin}} = \frac{12}{10} = 12 \ \Omega \tag{4.4}$$

and

$$R_{Lnom} = \frac{R_{Lmin} + R_{Lmax}}{2} = 6.6\ \Omega. \tag{4.5}$$

select R=6.8 Ω. The maximum, nominal and minimum value of DC voltage transfer function are

$$M_{VDCmin} = \frac{V_O}{V_{Imax}} = \frac{12}{32} = 0.38, \tag{4.6}$$

$$M_{VDCnom} = \frac{V_O}{V_{Inom}} = \frac{12}{28} = 0.43 \tag{4.7}$$

and

$$M_{VDCmax} = \frac{V_O}{V_{Imin}} = \frac{12}{24} = 0.50. \tag{4.8}$$

Assuming converter efficiency $\eta = 85$ % The minimum, nominal and maximum value of duty cycle are

$$D_{min} = \frac{M_{VDCmin}}{\eta} = \frac{0.375}{0.85} = 0.441, \tag{4.9}$$

$$D_{nom} = \frac{M_{VDCnom}}{\eta} = \frac{0.43}{0.85} = 0.506 \tag{4.10}$$

and

$$D_{max} = \frac{M_{VDCmax}}{\eta} = \frac{0.5}{0.85} = 0.588. \tag{4.11}$$

The minimum inductance required for the converter to operate in continuous conduction mode is given by

$$L_{min} = \frac{R_{Lmax}(1 - D_{min})}{2f_s} = \frac{12(1 - 0.411)}{(2 \times 10^5)} = 33.54\ \mu\text{H}. \tag{4.12}$$

Let $L = 100\ \mu$H. The maximum ripple in inductor current is

$$\Delta i_{Lmax} = \frac{V_O(1 - D_{min})}{f_s L} = \frac{12(1 - 0.441)}{(10^5 \times 100 \times 10^{-6})} = 0.67\ \text{A}. \tag{4.13}$$

The ripple voltage

$$V_r = \frac{V_O}{100} = \frac{12}{100} = 120\ \text{mV}. \tag{4.14}$$

The maximum DC resistance offered by the filter capacitance is

$$r_{Cmax} = \frac{V_r}{\Delta i_{Lmax}} = \frac{120 \times 10^{-3}}{0.67} = 0.18\ \text{m}\Omega. \tag{4.15}$$

Let $r_C = 50$ mΩ. The minimum value of filter capacitor is given by

$$C_{min} = \max\left\{\frac{D_{max}}{2f_s r_C}, \frac{1 - D_{min}}{2f_s r_C}\right\} = \frac{D_{max}}{2f_s r_C} = \frac{0.588}{2 \times 10^5 \times 50 \times 10^{-3}} = 58.8\ \mu\text{F}. \quad (4.16)$$

Pick $C = 220\ \mu$F/25 V/50 mΩ,

Voltage and current stresses are given by

$$V_{SMmax} = V_{DMmax} = V_{Imax} = 32\ \text{V} \quad (4.17)$$

and

$$I_{SMmax} = I_{DMmax} = I_{Omax} + \frac{\Delta i_{Lmax}}{2} = 10 + 1.6772 = 10.839\ \text{A}. \quad (4.18)$$

Knowing the values of inductor L, capacitor C, load resistor R and input voltage V_I, the circuit can be connected as shown in Figure 4.1. The MOSFET and diode can be selected based on their respective voltage and current stresses as shown in equations (4.17) and (4.18). An mtp12n10e as a MOSFET and an mur1540 as a diode is selected.

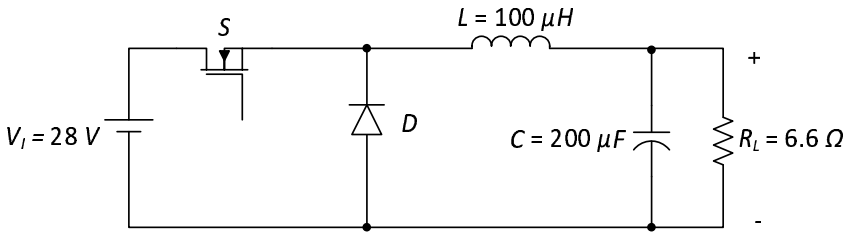

Figure 4.1: Circuit diagram of the buck DC-DC converter after implementing the design specification.

Now, to control this designed buck converter, it needs to be analyzed for its time and frequency responses to decide the required compensation. This can not be achieved by using linear circuit equations, for which a small-signal model is derived as discussed in Chapter 2. Using the transfer function T_i as given in equation (2.24) the magnitude and frequency response of the system can be plotted as shown in Figure

4.2, which for the selected specifications and equation (2.75) to (2.31) has a zero at $f_{zi} = 1.12$ kHz, conjugate poles at $f_o = 1.12$ kHz, damping factor of $\xi = 0.1514$ and quality factor of $Q = 3.316$ as shown in Figure 4.2. Taking an inverse laplace of this transfer function gives us the relation between the inductor current and the change in duty cycle, in time domain. Thus, step response can be plotted. Figure 4.3 represents the step response of average value of inductor current, when there is a step change in duty cycle from 0.5 to 0.7. One can note that the step response has high overshoots of 233%, a settling time and rise time of 3.9 ms and 0.0125 ms respectively. This can be improved upon my using a controller in a closed loop, which is dealt upon in the following section.

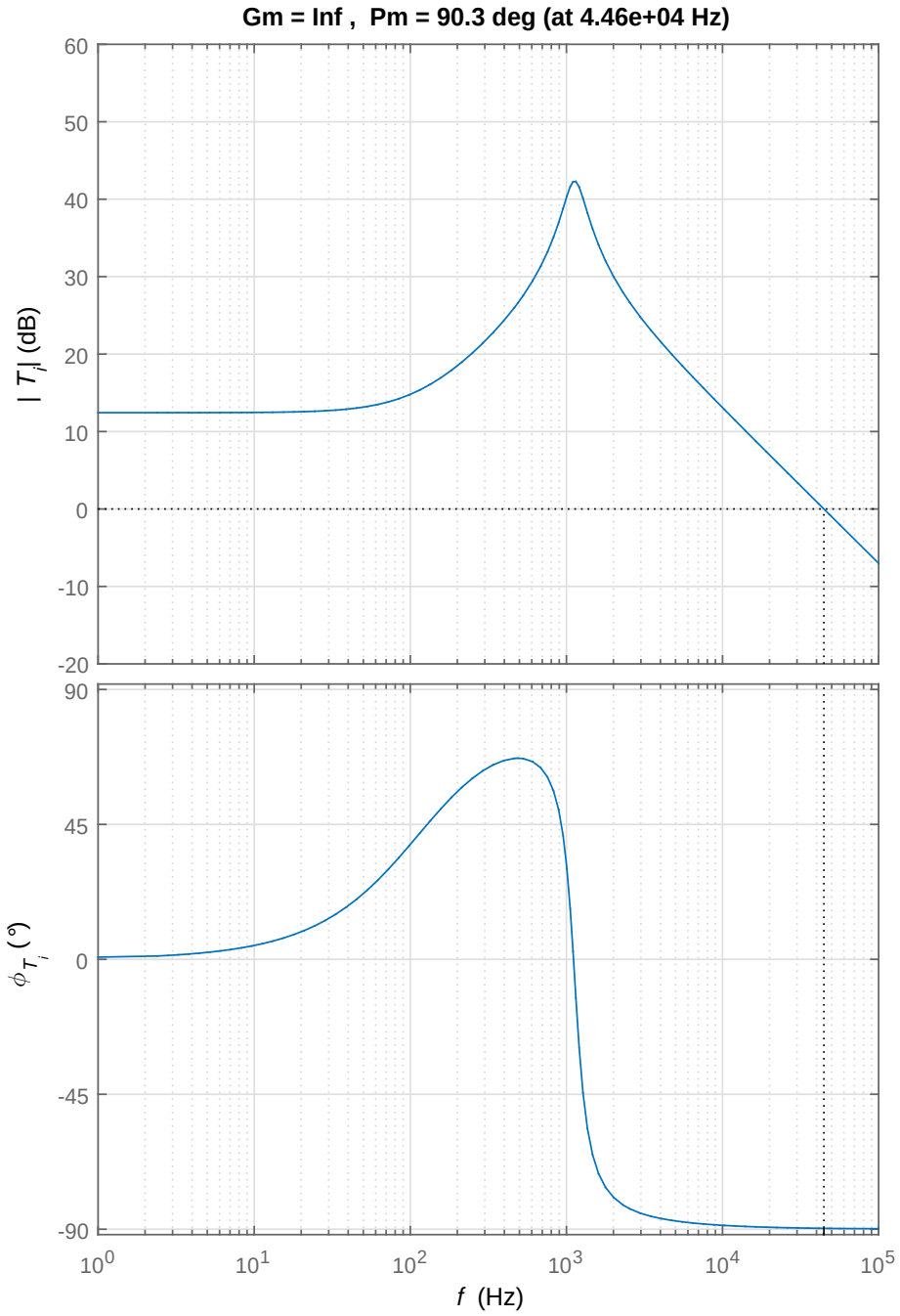

Figure 4.2: Magnitude and phase plots of control-to-inductor current transfer function of buck DC-DC converter.

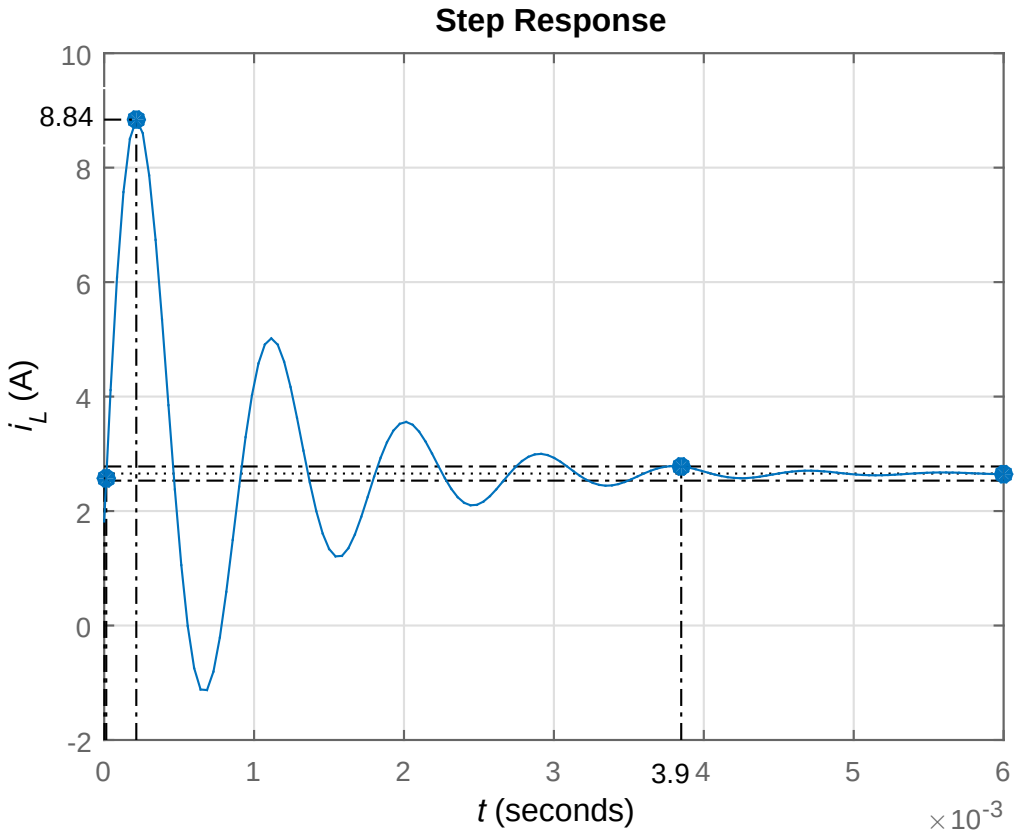

Figure 4.3: Step response of inductor current of buck DC-DC converter for a step change in duty cycle.

4.3 Closed-Loop Buck DC-DC Converter

To enable the converter to maintain a constant inductor current a closed loop can be implemented. Later the responses of the system can further be improved upon by adding controllers. To better comprehend the converter along with controller, a block diagram is represented in Figure 4.4. The inner most loop is the current control loop and the outer loop is the voltage control loop. Since the controller is now a part of the total closed loop system the properties of the controller can be designed in such a way that it improves any drawbacks closed loop buck DC-DC converter had without any controller compensation.

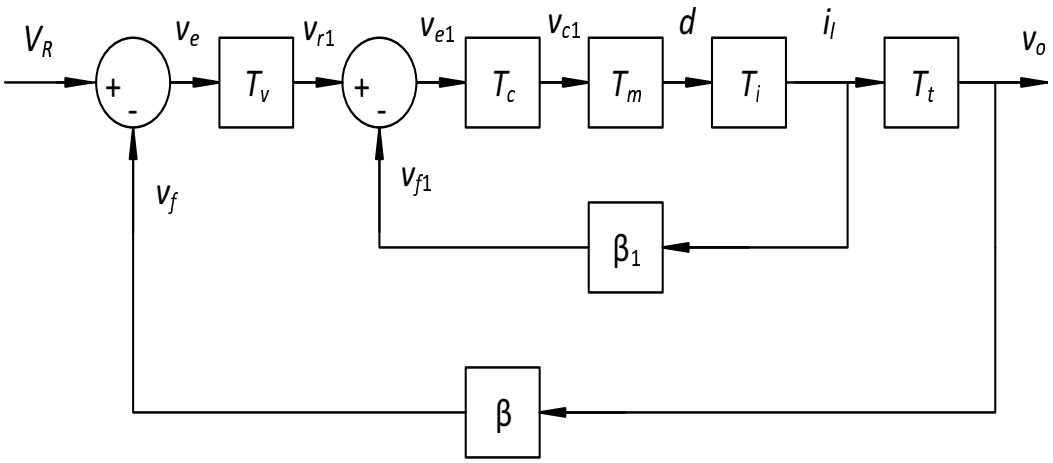

Figure 4.4: Block diagram of the DC-DC buck converter with inner current control loop and output voltage control loop.

In the block diagram

- T_i: Control-to-Inductor Current Transfer Function,
- T_m: Analog-to-Digital Conversion Gain,
- T_c: Inductor Current Controller Transfer Function,
- T_t: Output Voltage-to-Inductor Current Transfer Function,
- T_v: Output Voltage Control Transfer Function,
- β_1: Gain due to Sense Resistance,
- β: Voltage Feedback Gain.

The control-to-inductor current transfer function T_i and output voltage-to-inductor current transfer function have been derived in Chapter 2. β_1 is the gain due to sense resistance of the inner current loop, which senses the inductor current and converts it into a voltage so that it can be compared to another voltage reference v_{r1} using an op-amp. β is yet another sensor, which acts as a feedback loop for the outer

voltage loop. T_m is an analog to digital converter, which adds gain to the control loop. This converter contains an op-amp, which adds gain to the system. This gain is dependent of the amplitude on the reference voltage used and is given by $T_m = \frac{1}{V_{Tm}}$, where V_{Tm} is the amplitude of the reference voltage applied to the op-amp, which for this thesis is V_{Tm}=5 V. T_c and T_v are current and voltage controllers respectively. A circuit diagram representing the total control scheme with the converter can be seen in Figure 4.5. The design of the current-mode and voltage-mode controllers will be discussed in the further sections.

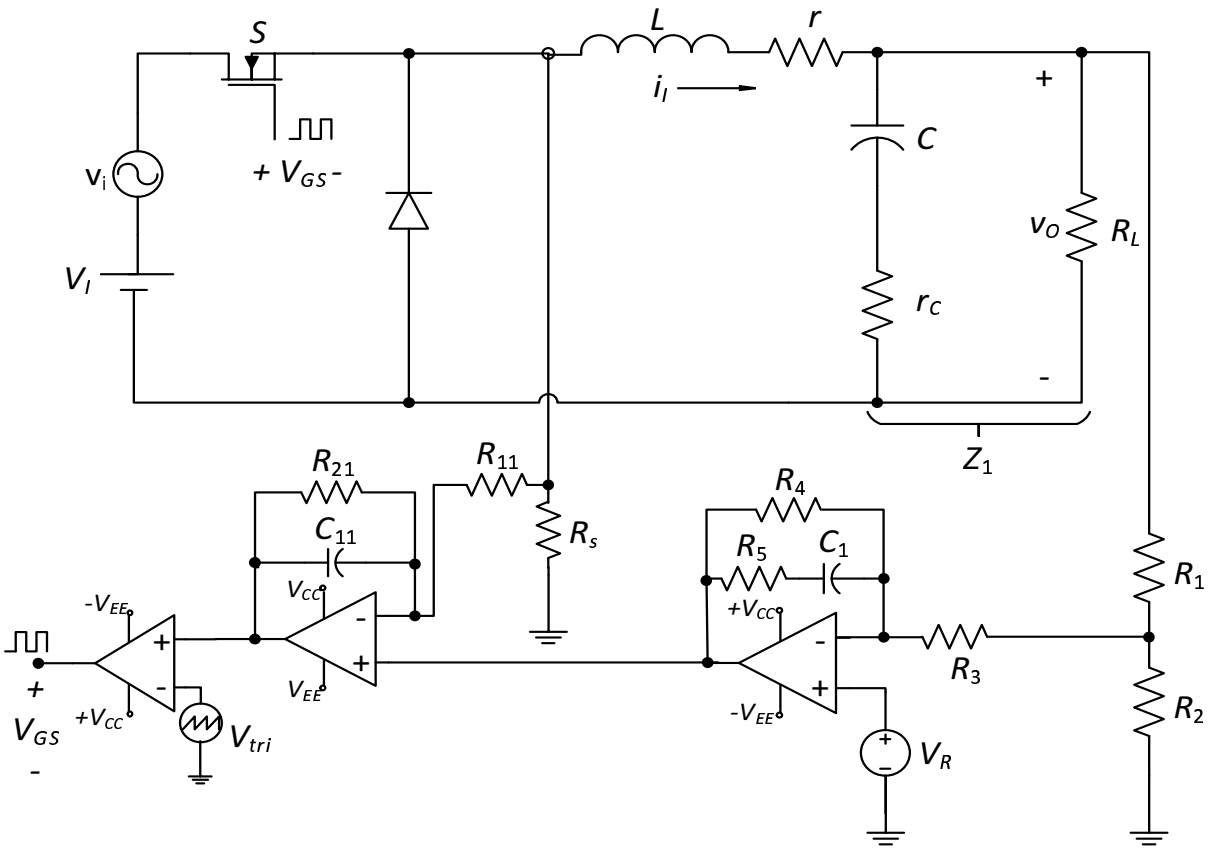

Figure 4.5: Circuit diagram of DC-DC buck converter with inner current control loop and output voltage control loop

4.3.1 Design of Inner Current Control-Mode-Controller

The open loop gain of the system can be seen in Figure 4.6. This provides an open loop relation between any change in the error voltage v_{e1} to the feedback voltage v_{f1}. First, the compensation provided by the controller is set equal to one and the loop gain $T_{k1}=\frac{v_{f1}}{v_{e1}}=T_m T_i \beta_1$ is plotted as shown in Figure 4.7. One can note that the response has a very low DC gain. This will make it difficult to track any change in the inductor current. Therefore, a controller with high DC gain is required.

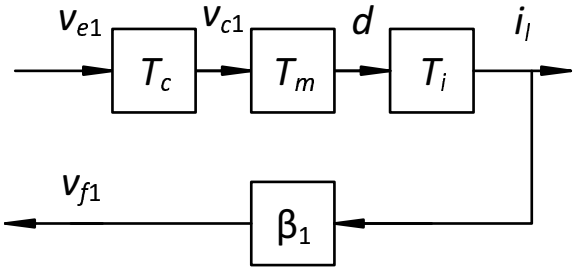

Figure 4.6: Block diagram of inner loop representing closed loop inductor current to control relationship

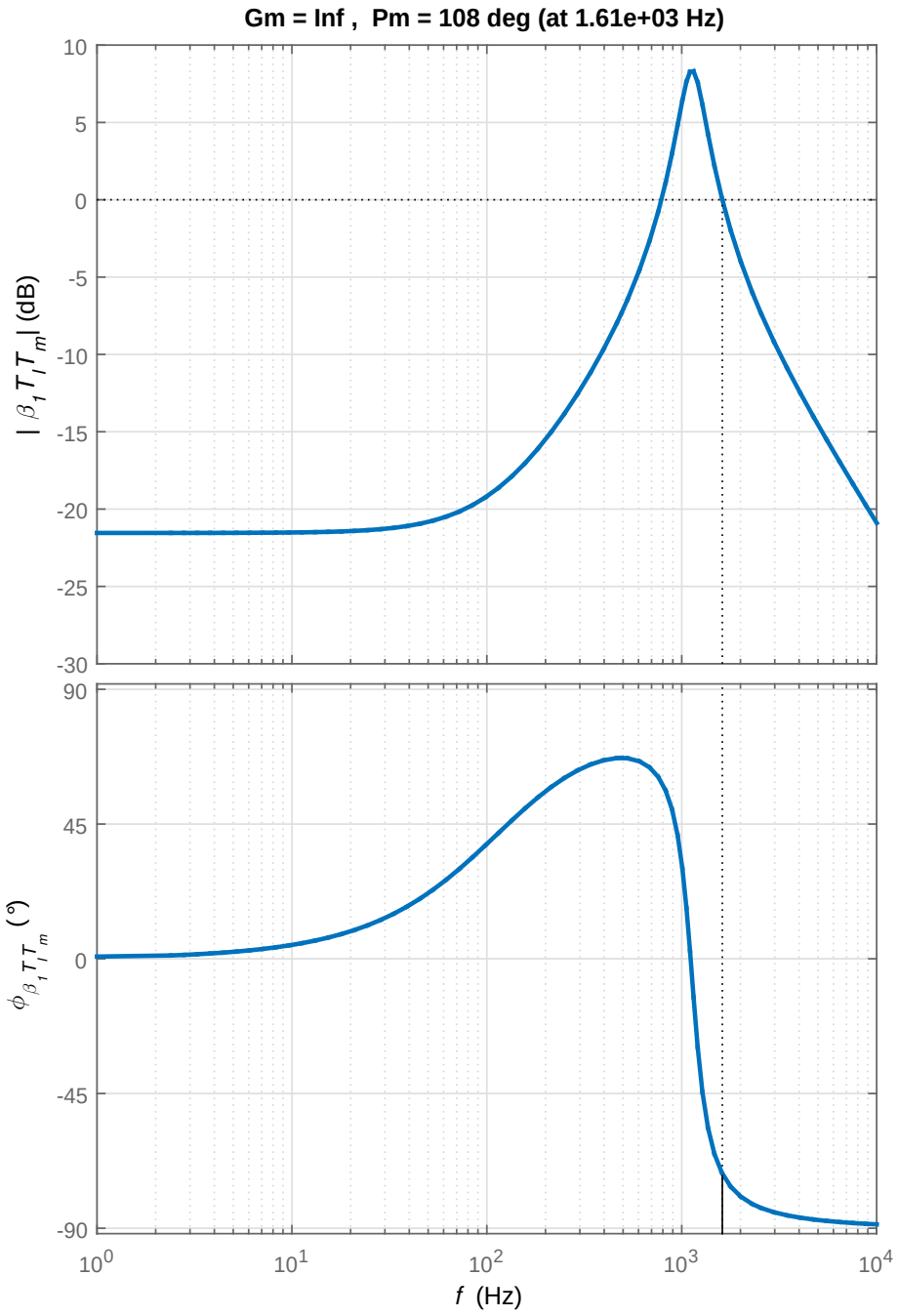

Figure 4.7: Magnitude and phase plots of internal loop gain without controller compensation.

It should also be kept in mind that the ripple in the inductor current needs to be attenuated to be able to use its average value as the control voltage. Therefore, a controller with a bandwidth enough to attenuate the inductor current ripples is required. Since, the ripples have a frequency equal to the switching frequency of the buck DC-DC converter, a controller with a crossover frequency less than the switching frequency of the converter can be used. Both the above mentioned criteria of the controller can be accomplished by using a first order type zero integral controller as shown in Figure 4.8. The values of R_{11}, R_{12} and C_{11} is derived on the basis of the controller requirement. The transfer function representing this controller can be derived as follow: From equation (3.1)

$$\frac{v_{c1}}{v_{f1}} = -\frac{Z_f}{Z_1}, \tag{4.19}$$

From Figure 4.8, the equation (3.1) can be written as

$$\frac{v_{c1}}{v_{f1}} = -\frac{R_{21}}{R_{11}\left[C_{11}s(R_{21} + \frac{1}{C_{11}s})\right]}, \tag{4.20}$$

$$\frac{v_{c1}}{v_{f1}} = -\frac{R_{21}}{R_{11}}\frac{1}{R_{21}C_{11}s + 1}, \tag{4.21}$$

$$T_c = -\frac{v_{c1}}{v_{e1}} = \frac{Z_f}{Z_i} = \frac{R_{21}}{R_{11}}\frac{1}{R_{21}C_{11}s + 1}, \tag{4.22}$$

$$T_c = \frac{1}{R_{11}C_{11}}\left(\frac{1}{s + \frac{1}{R_{21}C_{11}}}\right), \tag{4.23}$$

is the inner current mode controller transfer function. The DC gain is given by

$$T_c(0) = \frac{R_{21}}{R_{11}}. \tag{4.24}$$

Since the comparison between the average value of inductor current and reference voltage is required, the slope of the inductor current, when the switch turns off, given by $\frac{V_O}{L}$ must be less than the slope of the triangular control voltage to be able to

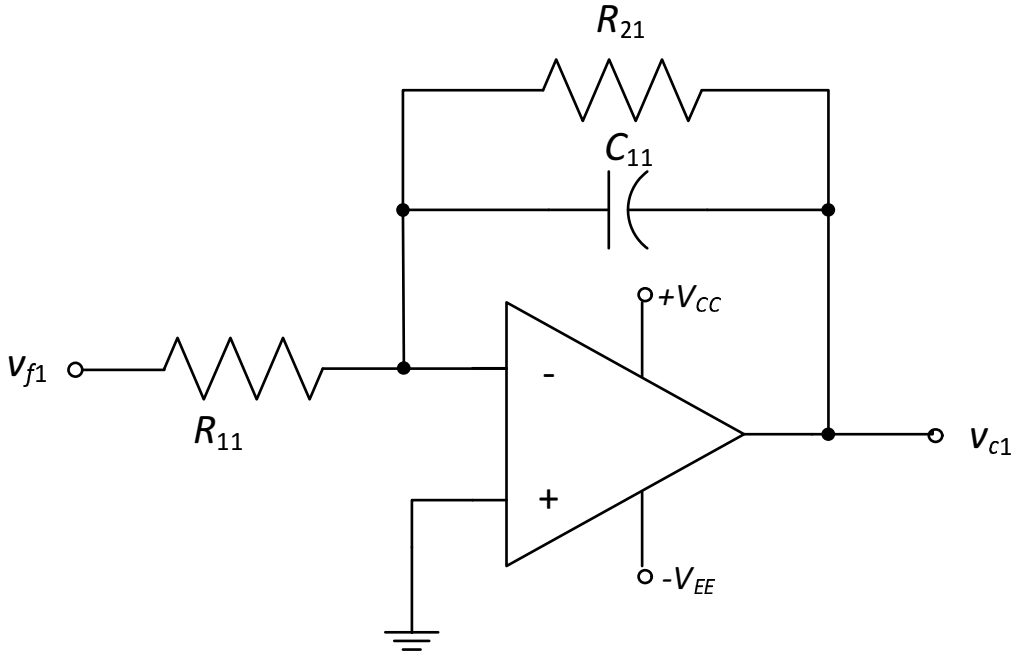

Figure 4.8: Circuit diagram of a first order type zero current mode controller

compare their average values [2].

Therefore,

$$V_{Tm} f_s = \beta_1 \frac{V_O}{L} \frac{R_{21}}{R_{11}}, \tag{4.25}$$

where $V_{Tm} f_s$ is the slope of the PWM control voltage, $\frac{V_o}{L}$ gives the downward slope of the inductor current, β_1 is the gain due to sense resistance and $\frac{R_{21}}{R_{11}}$ is the DC gain of the controller. For this control scheme, the inductor current is sensed using a sense resistance R_s as shown in Figure 4.5. The sensed resistance for this thesis is selected to be equal to 0.1 Ω. This sensed current is used to provide control voltage for a PWM generator. This PWM generator provides a pulse at the required duty cycle to drive the MOSFET.From equation (4.25),

$$\frac{R_{21}}{R_{11}} = \frac{L V_{Tm} f_s}{\beta_1 V_O}, \tag{4.26}$$

$$\frac{R_{21}}{R_{11}} = \frac{200 \times 10^{-6}(5)(100 \times 10^3)}{0.1(12)}, \tag{4.27}$$

$$\frac{R_{21}}{R_{11}} = \frac{500}{12}, \tag{4.28}$$

where $\frac{R_{21}}{R_{11}}$ is the DC gain of this controller. Hence, shows that the controller has a high DC gain. This will help compensate for the low DC gain for the open loop gain as seen in Figure 4.7. Now assuming $R_{11} = 1.2$ kΩ and from equation (4.28), we get $R_{12} = 50$ kΩ. Now knowing the values of R_{11} and R_{21}, magnitude and phase plots of $T_{CL} = T_m T_i T_c \beta_1$ can be plotted for different values of C_{11} to obtain phase margin of 60^0. From Figure 4.10 the magnitude and phase plots has a good phase margin of 59.4^0, which was obtained at $C_{11} = 60$ pF. Figure 4.9, represents the magnitude and phase plots of the controller. It can be noted from Figure 4.9 that the controller cut off frequency lies beyond the switching frequency of the buck DC-DC converter. Therefore, from equation (3.15) the ripples in the inductor current with frequency equal to the switching frequency of the buck converter do not get attenuated completely. Instead a small second order time varying control voltage is produced by the controller. The obtained values are plugged into saber to verify this current controller. This can be referred in the next chapter.

It can be seen from Figure 4.10 the loop gain with controller transfer function has a good DC gain thus helps in proper tracking of the change in the inductor current, while maintaining a good phase margin of 59.4^0 at 30 kHz.

Now, the reference voltage V_{R1}, which will be required to initiate and maintain the controller can be calculated by considering the DC gain of the current controller $\frac{R_{12}}{R_{11}}$. Since $V_{C1} = V_{Tm} D$.

$$V_{C1} = 5 \times 0.5 = 2.5 \text{ V}, \tag{4.29}$$

From equation (4.24)

$$T_c(0) = \frac{R_{21}}{R_{11}} = \frac{500}{12}, \tag{4.30}$$

the output of an op-amp with a non zero voltage at its non-inverting terminal as

shown in Figure 4.8 is given by,

$$V_{C1} = \frac{R_{11}}{R_{21}}(V_{R1} - V_{F1}) + V_{R1}, \tag{4.31}$$

the feedback voltage V_{F1} comes from the sensed inductor current and is given by $V_{F1} = \beta_1 I_L$ giving us

$$V_{C1} = \frac{R_{11}}{R_{21}}(V_{R1} - \beta_1 I_L) + V_{R1}, \tag{4.32}$$

$$V_{R1} = \frac{V_{C1} + \beta_1 I_L \dfrac{R_{11}}{R_{21}}}{1 + \dfrac{R_{11}}{R_{21}}} \tag{4.33}$$

Therefore, for the given specification

$$V_{R1} = \frac{0.241 \times 500}{512} = 0.2353\ V. \tag{4.34}$$

It is to be noted that the controller is designed for a crossover frequency more than the switching frequency of the converter. therefore, small oscillations in the control voltage is observed. But these oscillations are not significant and could still reliably be used as a control voltage.

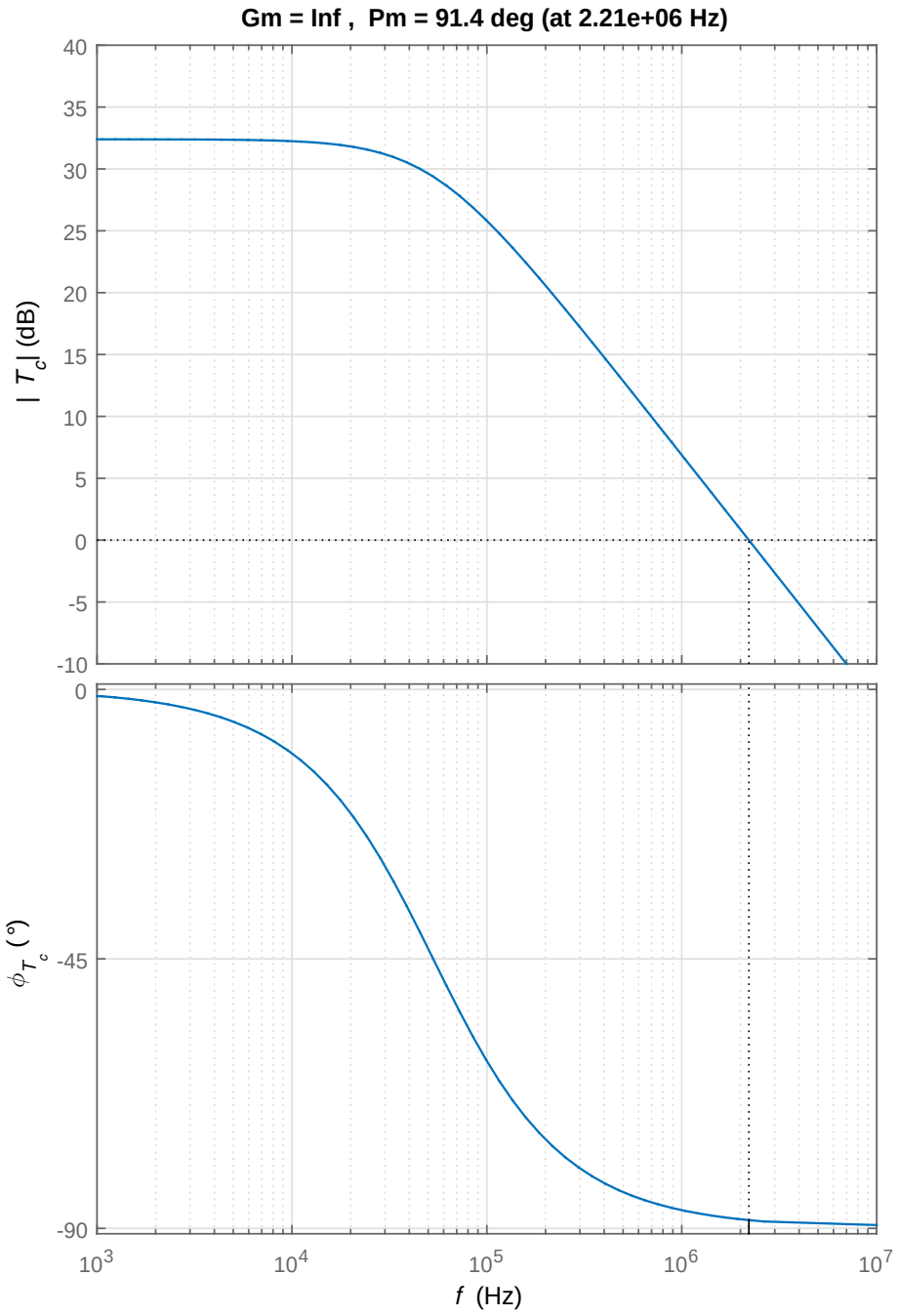

Figure 4.9: Magnitude and phase plots of average current mode controller

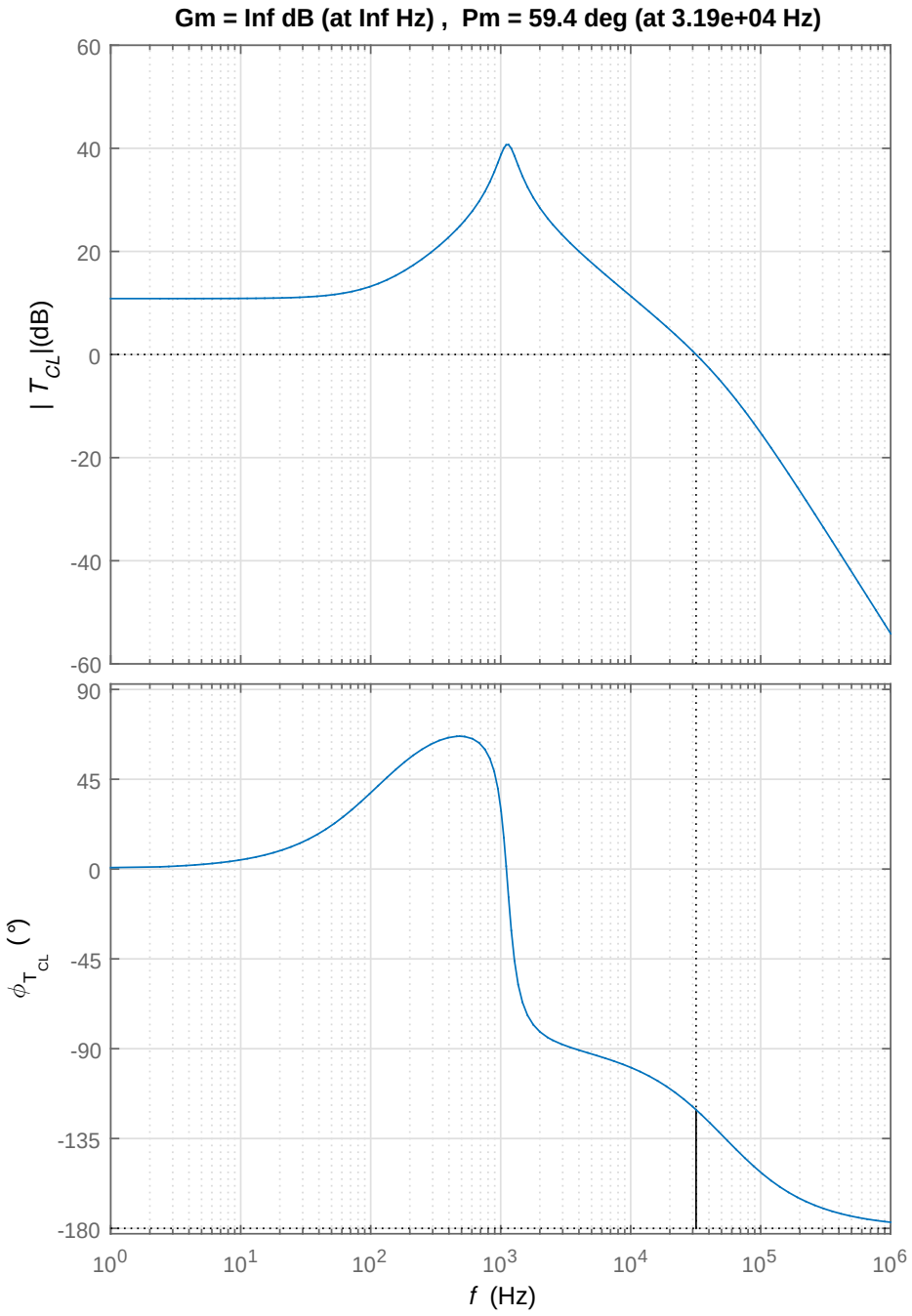

Figure 4.10: Magnitude and phase plots of inner loop gain with controller

The block diagram as shown in Figure 4.11 could also be used to find out the closed loop response of the system. The closed loop transfer function of the buck DC-DC converter with controller is given by

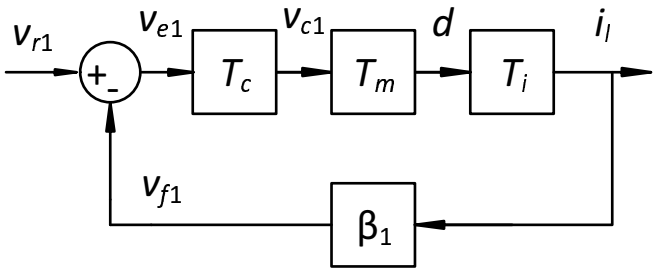

Figure 4.11: Block diagram of inner closed loop buck DC-DC converter.

$$T_{icl} = \frac{i_l}{v_{r1}} = \frac{T_c T_m T_i}{1 + T_c T_m T_i \beta_1}. \tag{4.35}$$

Taking the inverse laplace transform of (4.35), the step response can be plotted using MATLAB as shown in Figure 4.13. Here, the step change in reference voltage is from 0.23 V to 0.33 V.

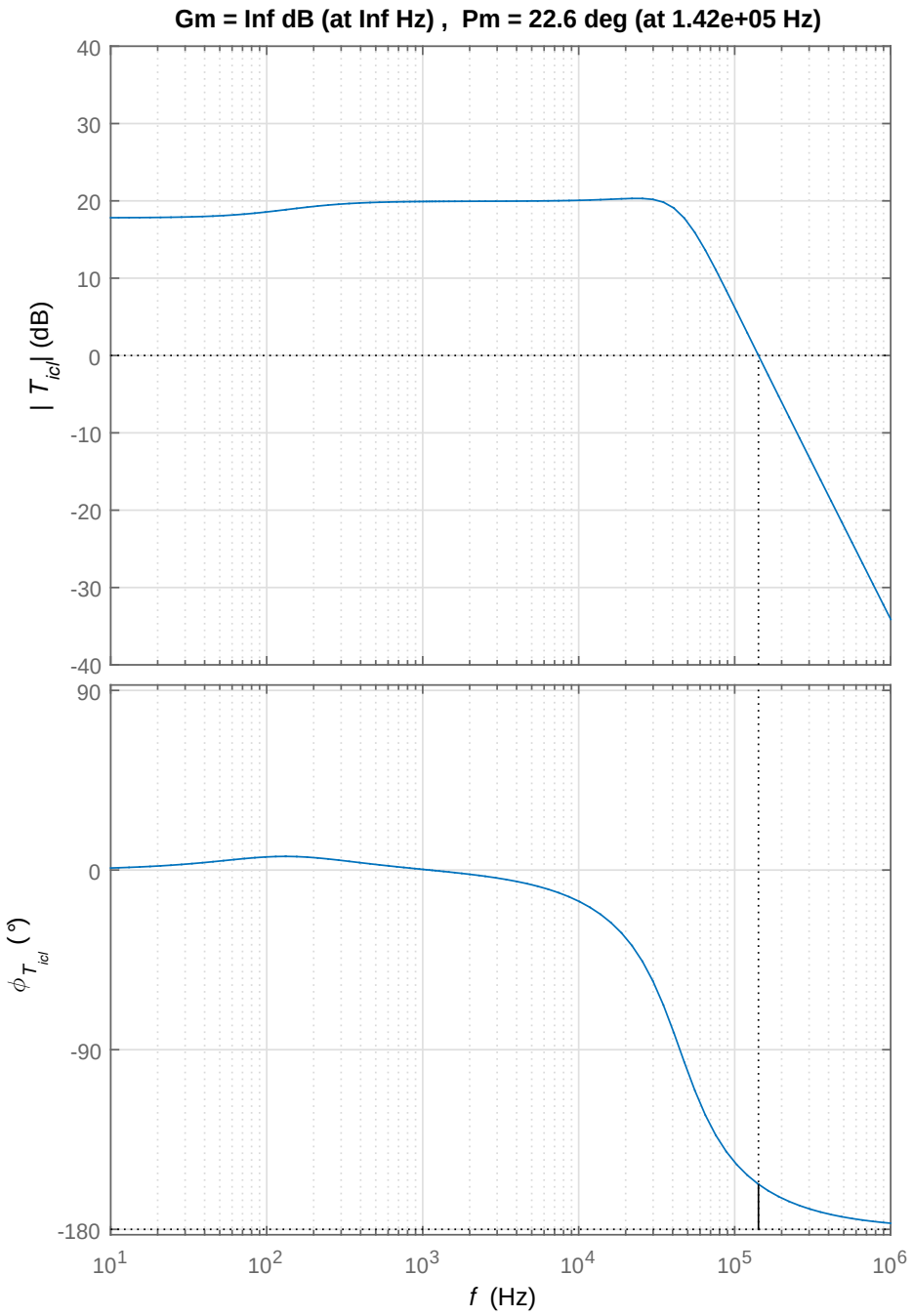

Figure 4.12: Magnitude and phase plots of closed loop control-to-inductor current transfer function of buck DC-DC converter.

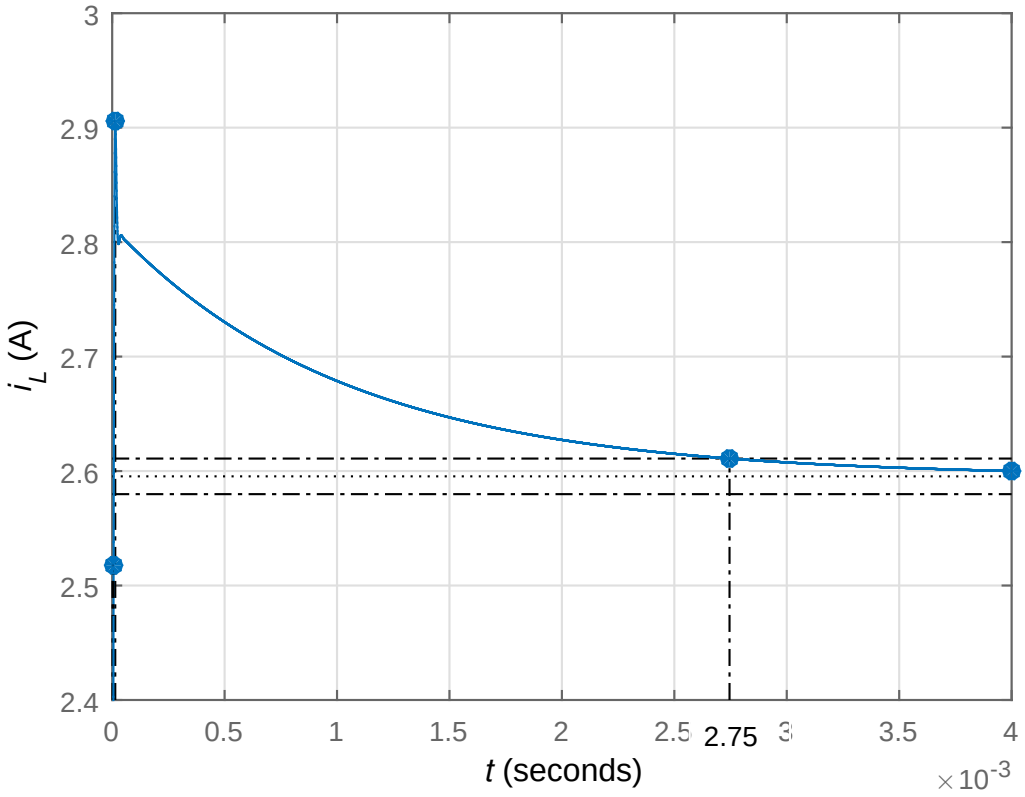

Figure 4.13: Step response of inductor current of a closed-loop buck DC-DC converter for a step change in duty cycle

It can be seen from Figure 4.13 that the overshoot is equal to 12% and the rise time and settling times are 4.9 μs and 2.75 ms, which when compared to an open loop system as shown in Figure 4.3 has a significant fall in overshoots and rise time. Thus making the system faster and also reducing surges duty to step change in duty cycle. the closed loop magnitude and phase plots can be seen in Figure 4.12

4.3.2 Design of Outer Voltage-Mode-Controller

A simple proportional controller could be used to control output voltage but using a PI controller makes the outer loop slower than the inner current loop. The controller can be seen in Figure 4.14. The transfer function of this controller can be calculated

as shown below.

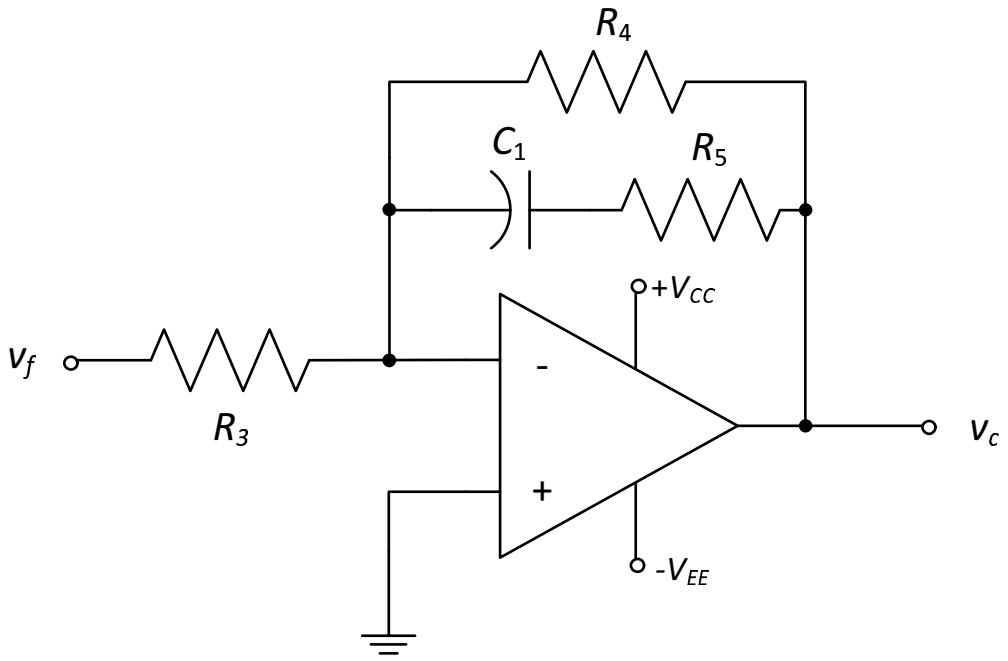

Figure 4.14: Circuit diagram representing PI controller for outer voltage loop control.

$$v_c = -\frac{Z_f}{Z_i} v_f, \tag{4.36}$$

$$v_c = -\frac{\dfrac{1}{\dfrac{1}{R_4} + \dfrac{1}{R_5 + \dfrac{1}{C_1 s}}}}{R_3} v_f, \tag{4.37}$$

$$v_c = -\frac{\dfrac{1}{\dfrac{1}{R_4} + \dfrac{C_1 s}{C_1 R_5 s + 1}}}{R_3} v_f, \tag{4.38}$$

$$v_c = -\frac{\dfrac{R_4(C_1 R_5 s + 1)}{C_1 R_5 s + R_4 C_1 s + 1}}{R_3} v_f, \tag{4.39}$$

$$v_c = -\frac{R_4 C_1 R_5}{R_3 C_1 (R_5 + R_4)} \frac{s + \dfrac{1}{C_1 R_5}}{s + \dfrac{1}{C_1 (R_5 + R_4)}} v_f, \tag{4.40}$$

$$v_c = -\frac{R_4 R_5}{R_3(R_5+R_4)} \frac{s + \dfrac{1}{C_1 R_5}}{s + \dfrac{1}{C_1(R_5+R_4)}} v_f, \tag{4.41}$$

$$\frac{v_c}{v_f} = -\frac{R_4 R_5}{R_3(R_5+R_4)} \frac{s + \dfrac{1}{C_1 R_5}}{s + \dfrac{1}{C_1(R_5+R_4)}}, \tag{4.42}$$

which gives the voltage controller transfer function

$$T_v = -\frac{v_c}{v_f} = \frac{R_4 R_5}{R_3(R_5+R_4)} \frac{s + \dfrac{1}{C_1 R_5}}{s + \dfrac{1}{C_1(R_5+R_4)}}. \tag{4.43}$$

The DC gain is given by

$$T_v(0) = \frac{R_4}{R_3}. \tag{4.44}$$

For a good bandwidth, a gain of 15 is chosen. From equation (4.44),

$$\frac{R_4}{R_3} = 15, \tag{4.45}$$

select R_3=1000 Ω, that give R_4= 15000 Ω. The outer loop gain block diagram can be seen in Figure 4.15. Now for different values of C_1, the loop gain with controller compensation, given by $T_{VL} = T_v \dfrac{T_c T_i T_m}{1 + \beta_1 T_c T_i T_m} T_t \beta$ is plotted for a phase margin of 60^0. At $C_1 = 1$ nF, a good phase margin of 63.7^0 is obtained. This capacitance is selected and simulated on saber, which can be observed in next the chapter.

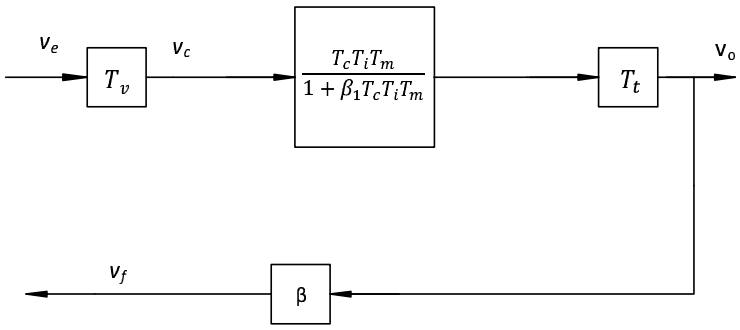

Figure 4.15: Block diagram representing outer loop gain

To initiate the controller and maintain the system output voltage a DC reference voltage V_R is required and needs to be calculated. For an op-amp with a non-inverting pin connected to V_R. The output of the controller is given by

$$V_C = V_R + T_v(0)(V_R - V_F), \tag{4.46}$$

form equation (4.44), for a low frequency

$$V_C = V_R + \frac{R_4}{R_3}(V_R - V_F), \tag{4.47}$$

where $\frac{R_4}{R_3}$ is the DC gain of the voltage controller. Since, for the inner current loop we need $V_{R1} = 0.24$ V, from equation (4.33). $V_C = V_{R1} = 0.24$ V. Therefore,

$$V_C = \frac{R_4}{R_3}(V_R - V_F) + V_R, \tag{4.48}$$

$$V_R = \frac{V_C + V_F \frac{R_4}{R_3}}{\frac{R_4}{R_3} + 1}, \tag{4.49}$$

$$V_R = \frac{0.24 + (1.2)(15)}{16} = 1.14 \text{ V}, \tag{4.50}$$

The block diagram as shown in Figure 4.17 could used to find out the closed loop frequency response. The closed loop transfer function of the buck DC-DC converter

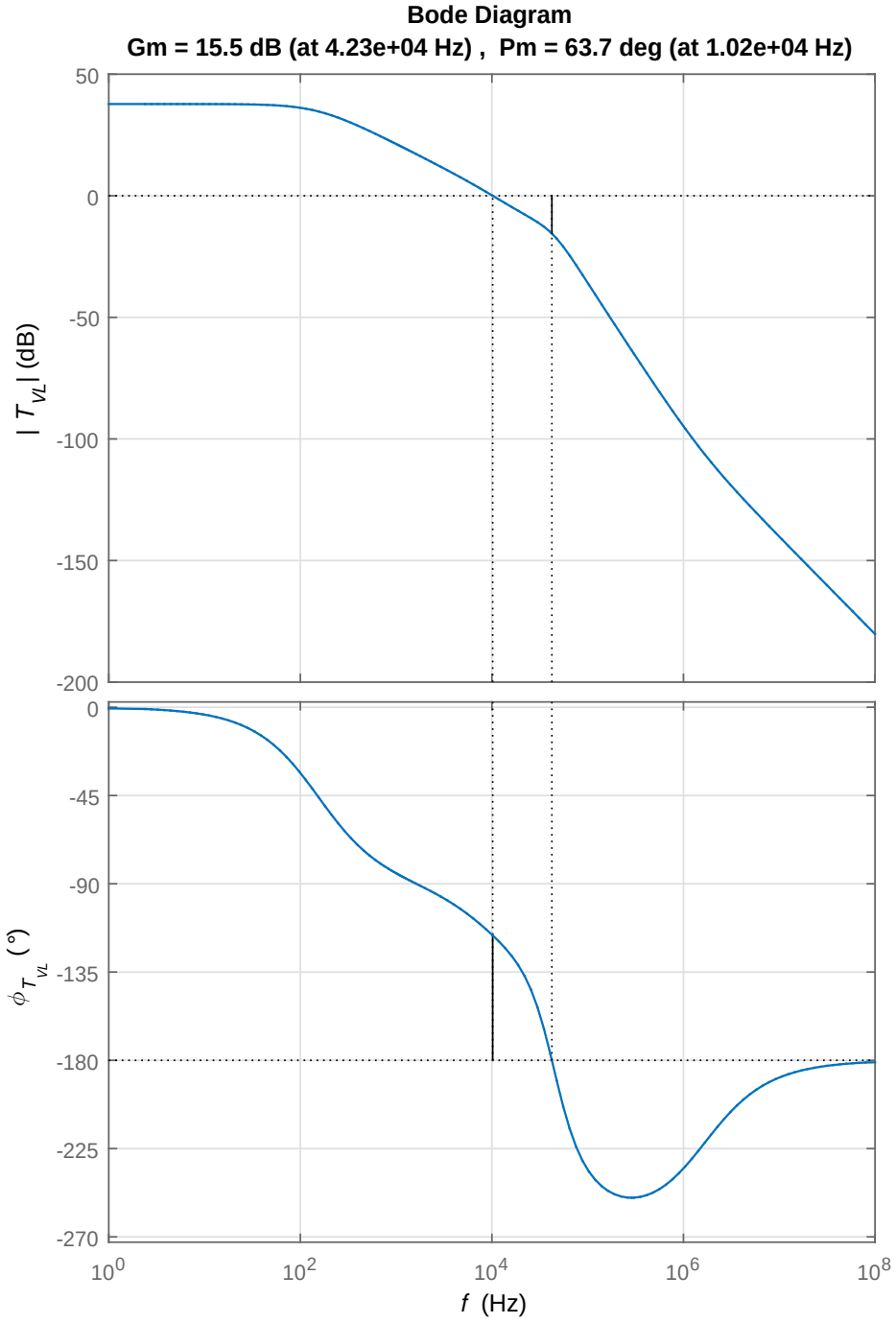

Figure 4.16: Magnitude and phase plots of outer loop gain with controller.

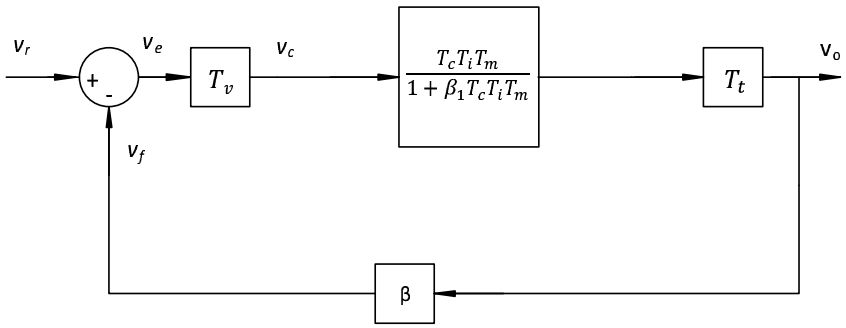

Figure 4.17: Block diagram for closed loop gain of outer voltage loop control.

with controller is given by

$$T_{ivl} = \frac{v_o}{v_r} = \frac{T_v T_{icl}}{1 + T_v T_{icl} \beta}. \tag{4.51}$$

The inverse laplace of (4.51) provides us with the time domain response of output voltage. The step response of the output voltage for a step change in refrence voltage can be plotted using MATLAB as shown in Figure 4.19. The closed loop frequency response can be seen in Figure 4.18.

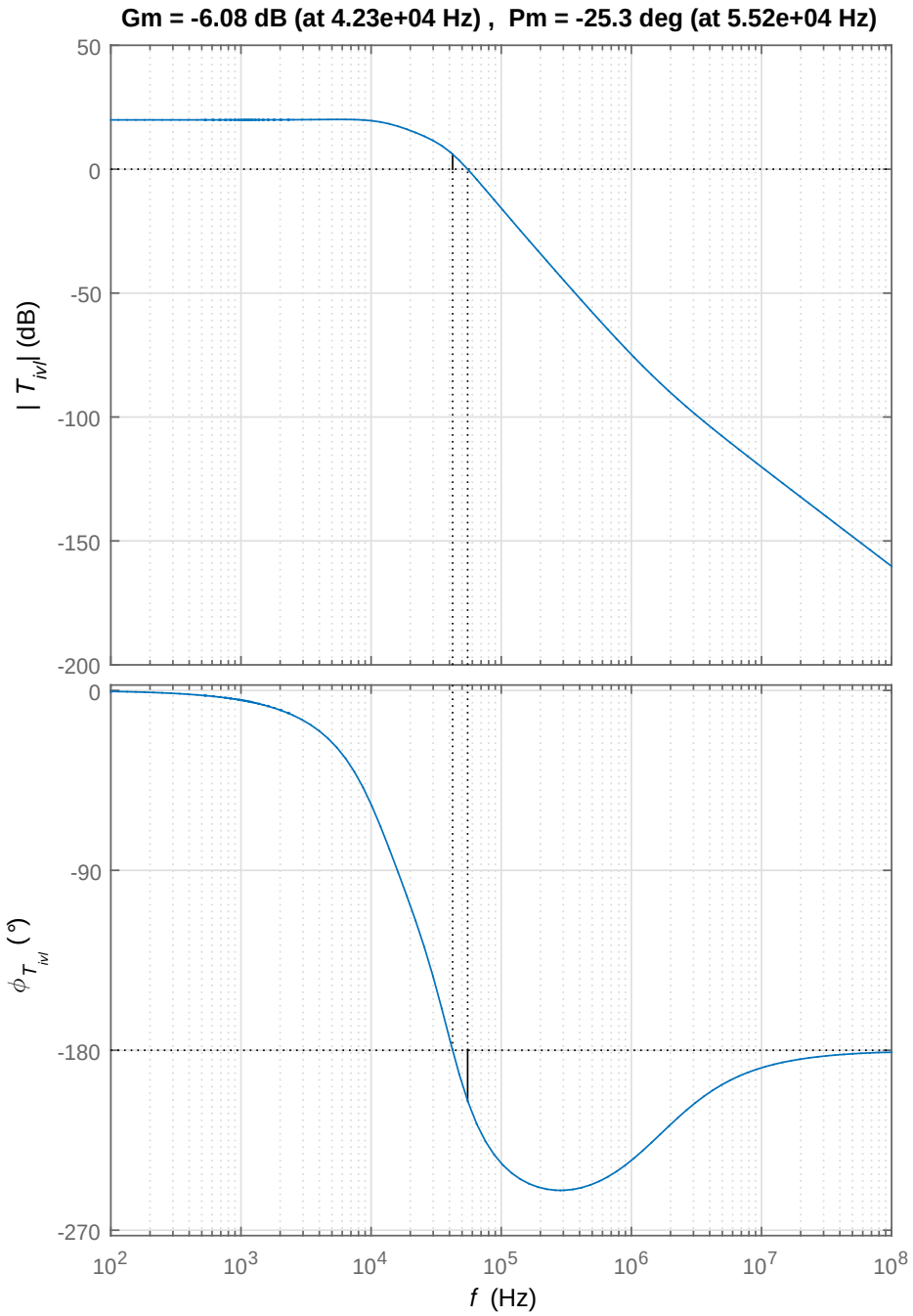

Figure 4.18: Magnitude and phase plots of outer closed loop gain with controller.

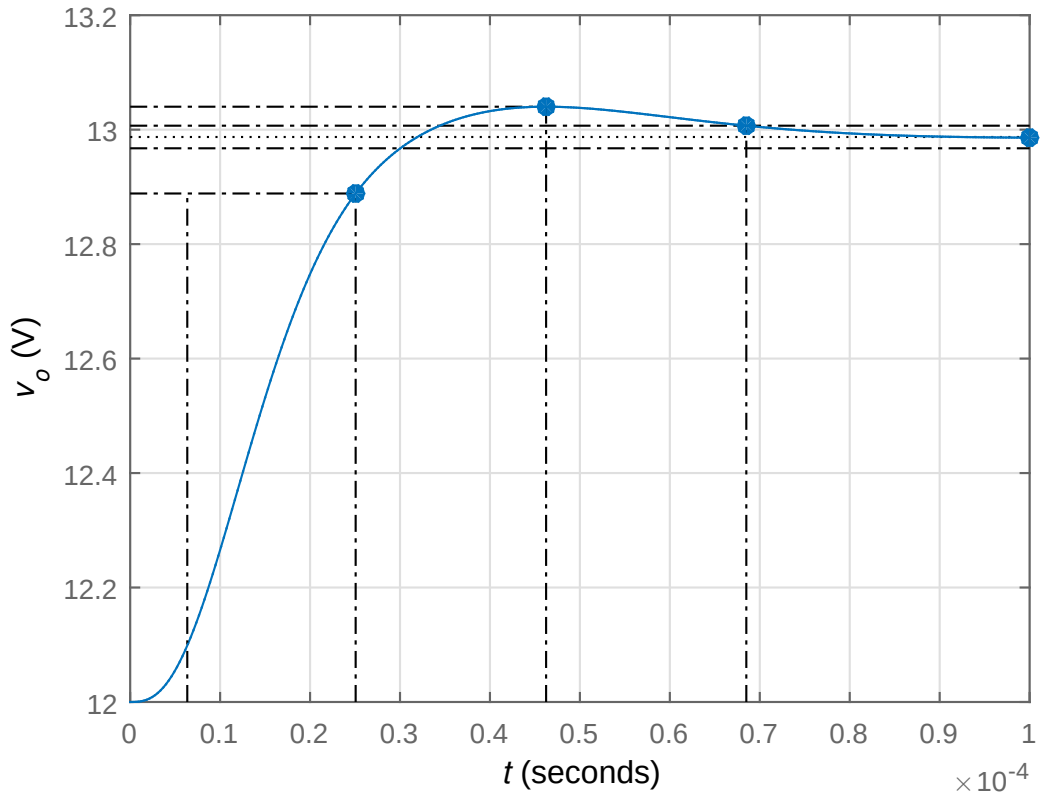

Figure 4.19: Step response of outer closed loop with controller.

It can be seen from Figure 4.19 that the system has a low overshoot of 0.4 %, rise and settling time of 18 μs and 68.5 μs giving us a response system with less overshoot.

5 Saber Simulations and Results

5.1 Introduction

Synopsys saber is a proven platform for modeling and simulating many physical systems. It is a user friendly platform, which provides full-system prototyping. Many virtual power electronic circuits can be connected and dynamic responses can be obtained in this interface. The designed controllers along with the buck DC-DC converter can be connected in saber and simulated for its dynamic responses. In this chapter the controller is tested for the change in load resistance, input voltage and the controller reference voltage.

5.2 Dynamic Response of Inner Current Control Loop

Circuit diagram of the buck DC-DC converter with inner current control loops connected on saber and can be seen in Figure 5.1. This circuit is simulated by added forced perturbations in the inductor current by varying load resistance, input voltage and reference voltage after time $t = 15$ ms. For each of these changes the steady state and transient responses of the inductor current is noted to know the controller properties.

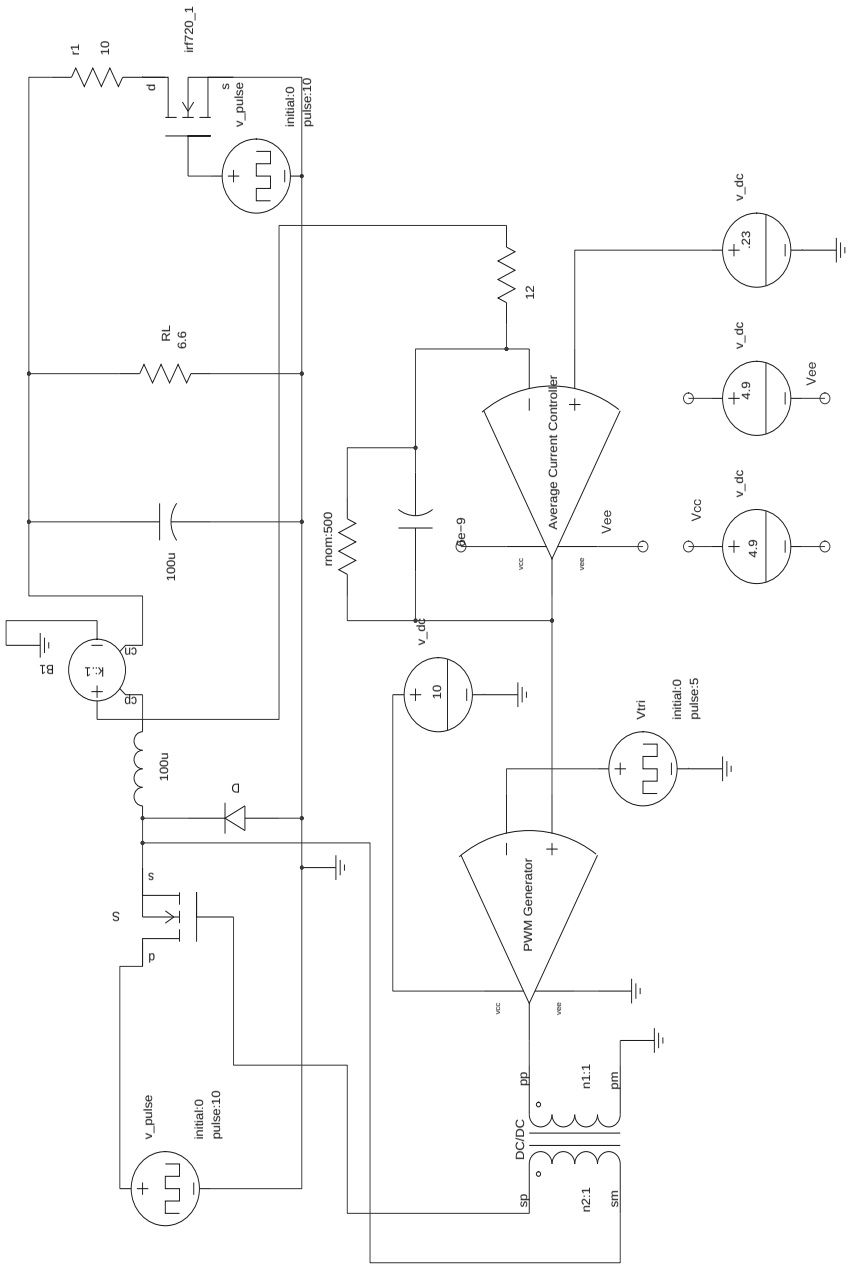

Figure 5.1: Saber circuit for average current mode control of inductor current.

5.2.1 Controller Response

As mentioned earlier the average current mode controller designed eliminates the ripples from the sensed inductor current to provide the average value at the controller output. Any error in the average value of the sensed inductor current will be amplified and will be used for controlling the buck DC-DC converter. Figure 5.2 represents the control voltage V_{C1} and the triangular reference voltage of PWM V_{tri}. It can be seen that the control voltage is not a pure DC but contains ripples, which are at a phase difference, with the sensed inductor current. This can be eliminated by using high capacitance in the feedback of the controller as shown in Figure 5.3. But doing so will cause the bandwidth of the closed loop control-to-inductor current T_{icl} to fall. It can also be noted that in both cases, the control voltage provides almost the same duty cycle, this is because the phase difference of the control voltage is almost equal to 90^0 hence the point of intersection of the control voltage with reference voltages are equal in both cases. But a low capacitance is selected in the feedback as it provides high T_{icl} bandwidth.

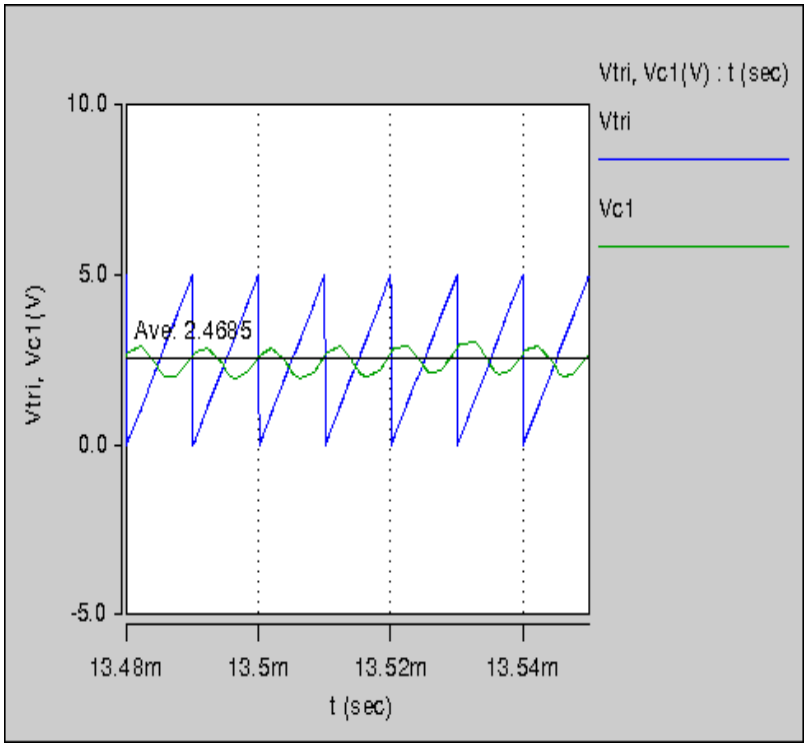

Figure 5.2: Waveforms representing control and sawtooth reference voltages for a good phase margin.

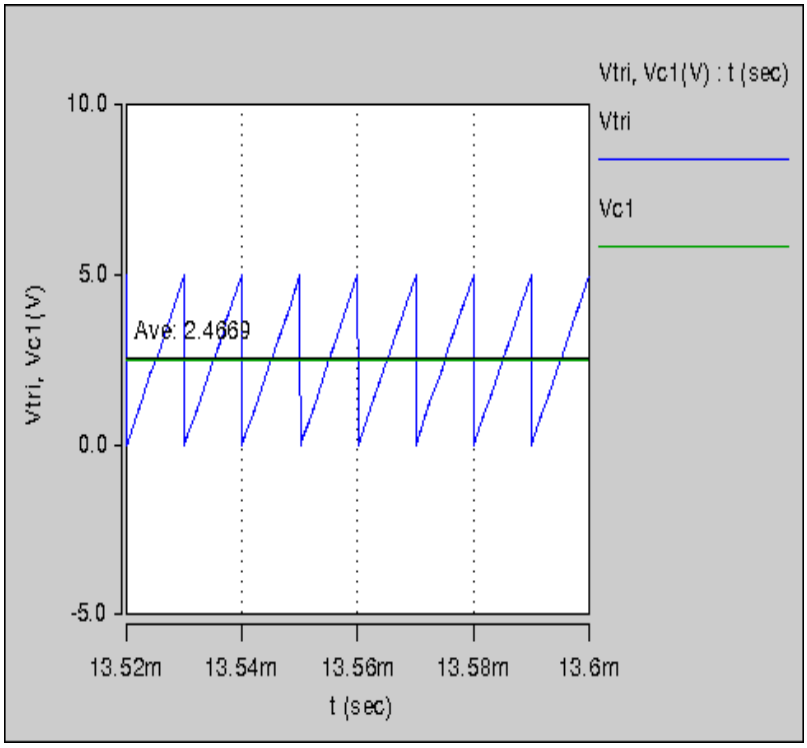

Figure 5.3: Waveforms representing control and sawtooth reference voltage with high capacitance in the feedback of the controller.

5.2.2 Dynamic Response of the Buck DC-DC Converter with Inner Current Control Loop for the Step Change in Load Resistance

From Figure 5.1, the controller senses for any change in the inductor current, when the load has changed and provides required compensation to nullify the change in the inductor current and maintain constant inductor current. But because of the change in load, the output voltage falls, which can also be seen in Figure 5.4.

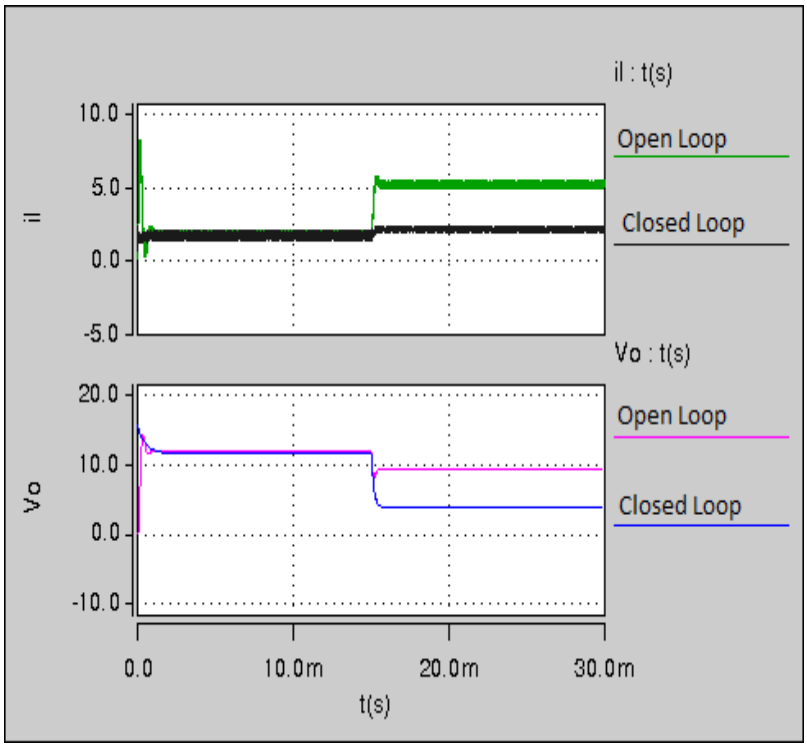

Figure 5.4: Waveforms representing inductor current and output voltage of the buck DC-DC converter for a step change in load resistance.

5.2.3 Dynamic Response of the Buck DC-DC Converter with Inner Current Control for the Step Change in Input Voltage

For a perturbation in the input voltage the inner current loop provides the required compensation even before this disturbance can reach the load at the output. Hence, also controlling the output voltage in the process. The waveforms of the inductor current and the output voltage for the step change in the input voltage can be seen

in Figure 5.5

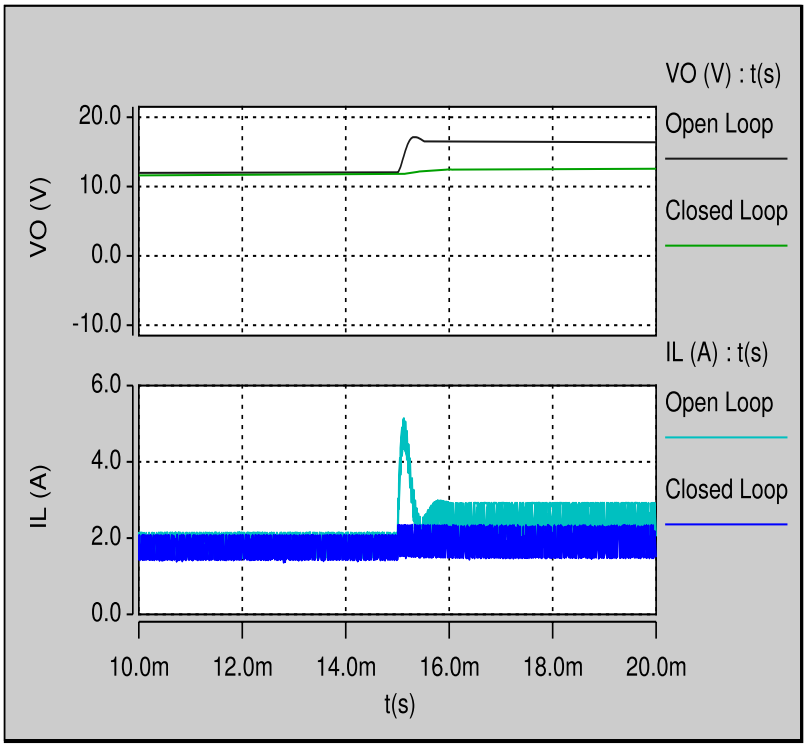

Figure 5.5: Waveforms representing inductor current and output voltage of the buck DC-DC converter for a step change in input voltage.

5.3 Dynamic Response of Outer Voltage Control Loop

Using the values obtained on MATALB, saber circuit is connected and as shown in Figure 5.6. One can note the output voltage for the designed buck converter in Figure 5.7. Here, the output voltage is $12V$, which satisfies our designed requirement. This designed buck DC-DC converter is made to pass through dynamic change in load resistance, input voltage and reference voltage, for which the responses of the inductor current and output voltage is noted.

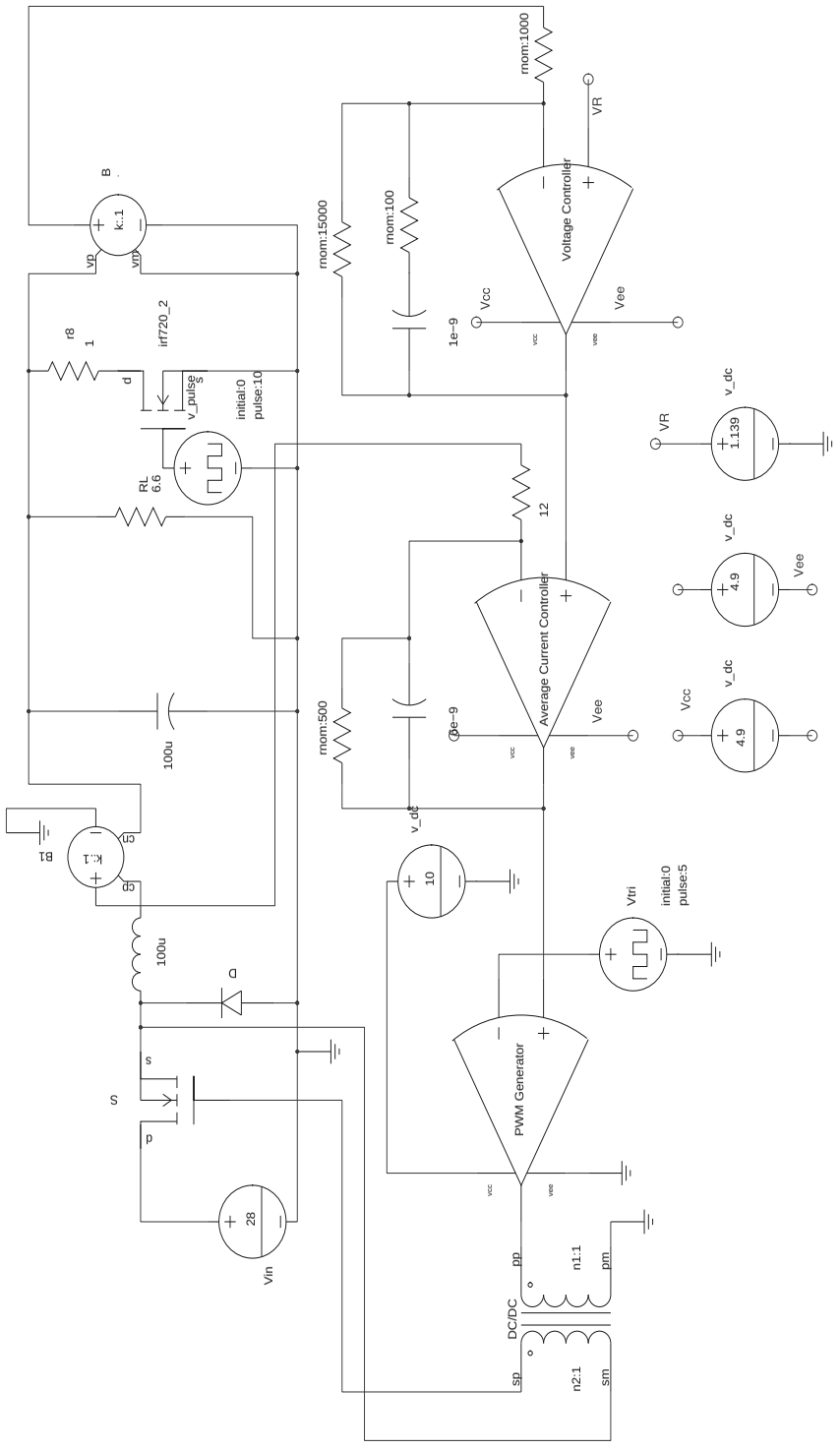

Figure 5.6: Saber circuit of a buck DC-DC converter with both inner current control and outer voltage control.

5.3.1 Dynamic Response of the Buck DC-DC Converter with Inner Current and Outer Voltage Control Loop for the Step Change in Load Resistance

It can be seen from Figure 5.7, when the load resistance falls down the output voltage still remains constant . Since the main aim of this controller is to obtain a constant output voltage the aim is fulfilled. Using an inner current loop provides a high degree of control and therefore the steady state error is very low.

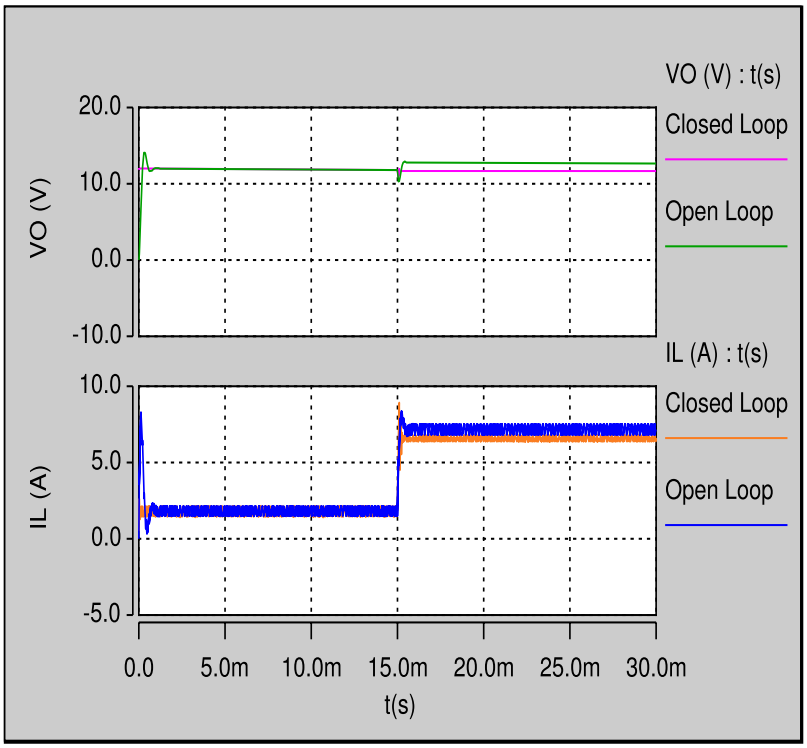

Figure 5.7: Waveforms of inductor current and output voltage of the buck DC-DC converter for a step change in load resistance.

5.3.2 Dynamic Response of the Buck DC-DC Converter with Inner Current and Outer Voltage Control Loop for the Step Change in Input Voltage

It can be noted from Figure 5.5 that, when the input voltage was stepped up by 10 V, the current control loop provided maximum compensation and prevented the disturbance to reach the output voltage. This has been improved upon by adding

an outer voltage loop, which has decreased the steady state error even further and this can be noted in Figure 5.8, where the steady state error of the output voltage has completely been nullified. Also, using a current control loop made sure that the average inductor current has also been maintained to a required value providing multiple signal control in the circuit.

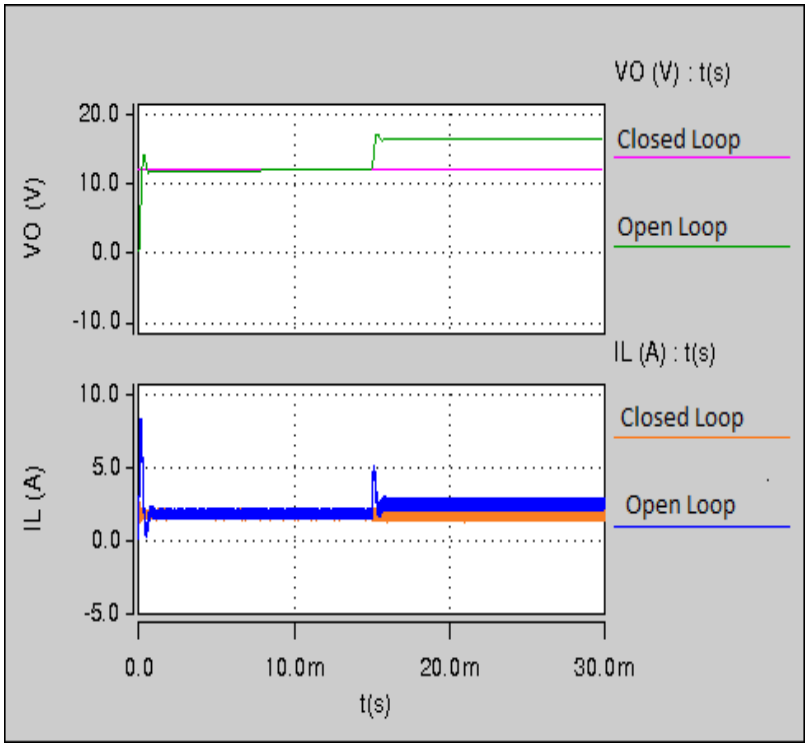

Figure 5.8: Waveforms of inductor current and output voltage of the buck DC-DC converter for a step change in input voltage.

6 Conclusion

6.1 Summary

- A current mode controller provides a higher order of control when compared to voltage mode controller.
- Using circuit averaging technique a small signal model of a non-linear system can be obtained
- A small signal model can be used to obtain linear transfer functions between you required quantities.
- Peak, valley, average are few example of different types of controllers available. They are named based on the characteristic of the sensed signal the controller manipulates for its control action.
- Since, average current mode controller averages out any high frequency disturbances it is preferable for power factor correction circuits.

6.2 Future Work

A first order buck DC-DC converter was designed in this thesis as the buck converter did not required a higher order controller transfer function. But, many different higher order average current mode controllers can still be designed depending on the system to which the controller is to be implemented. Further more this average current mode controller was implemented to average out the sensed inductor current. But, if the transfer function which related the switch current of the buck DC-DC converter to the control voltage is derived then the switch could directly be controlled. Here even though the switch has discontinuous current the controller will average it out and provide with a good control signal.

7 Bibliography

References

[1] Jorge Alberto Morales-Saldaña, Jesús Leyva-Ramos, Enrique Eduardo Carbajal-Gutiérrez, and Ma. Guadalupe Ortiz-Lopez "Average Current-Mode Control Scheme for a Quadratic Buck Converter With a Single," *IEEE Transactions on Power Electronics*, Vol. 23, No. 1, pp. 485-490, January 2008.

[2] Lloyd Dixon, "Average Current Mode Control of Switching Power Supplies," Unitrode Power Supply Design Seminar, pp. 356-369, 1990.

[3] Jian-Min Wang, Sen-Tung Wu, Yanfeng Jiang, Huang-Jen Chiu "A Dual-Mode Controller for the Boost PFC Converter," *IEEE Transactions on Industrial Electronics*, Vol. 58, No. 1, pp. 369-372, January 2011.

[4] Kashif Habib, Aftab Alam, Shahbaz Khan,"Average Current Control Mode Boost Converter for the Tuning of Total Harmonic Distortion Power Factor Correction using PSIM," Global Journal of Researches in Engineering: Electrical and Electronics Engineering, Vol. 14, Issue 5, Version 1.0, Year 2014.

[5] M. K. Kazimierczuk, *Pulse-Width Modulated DC-DC Power Converters*, John Wiley and Sons: UK, 2^{nd} Edition, 2016.

[6] Farid Golnaraghi, Benjamin C.Kuo, *Automatic Control Systems*, Ninth Ed., John Wiley and Sons: USA, 2009.

[7] Kiam Heong Ang, Gregory Chong, Yun Li, "PID Control System Analysis, Design, and Technology, "*IEEE Transactions on Control Systems and Technology*, Vol. 13, No. 4, pp. 559-576, July 2005.

[8] W. Tang, F. C. Lee, R. B. Ridley, "Small-Signal Modeling of Average Current-Mode Control," publication No. 0-7803-0485-3/92, *IEEE Trans. on Power Electronics*, vol. 8, no.2, pp. 112-119 April 1993.

[9] J. Leyva-Ramos, M.G. Ortiz-Lopez, L.H. Diaz-Saldierna, M. Martinez-Cruz, "Average current controlled switching regulators with cascade boost converters," *IET Power Electronics.*, 2011, Vol. 4, Iss. 1, pp. 1-10.

[10] Shamim Choudhury, "Average Current Mode Controlled Power Factor Correction Converter using TMS320LF2407A," *Digital Power, C2000 DSP and System Power Management*, pp. 1-14, July 2005.

[11] Robert Sheehan, "Understanding and Applying Current-Mode Control Theroy," *Power Electronics Technology Exhibition and Conference*, November 2007.

[12] Yingyi Yan, Fred C. Lee, Paolo Mattavelli, Pei-Hsin Liu, "I^2 Average Current Mode Control for Switching Converters," *IEEE Transactions on Power Electronics*, Vol. 29, No. 4, April 2014.

[13] J. G. Kassakian, J. M. Miller, and N. Traub, "Automotive electronics power up," *IEEE Spectrum*, vol. 37, pp. 34-39, 2000.

[14] Ali Aminian, Marian Kazimierczuk *Electronic Devices: A Design Approach*, Pearson Prentice Hall, c2004